

# Tightening convex relaxations of trained neural networks: a unified approach for convex and S-shaped activations

Pablo Carrasco<sup>1</sup> and Gonzalo Muñoz<sup>2\*</sup>

<sup>1</sup>Engineering School, Universidad de O'Higgins, Rancagua, Chile.

<sup>2\*</sup>Industrial Engineering Department, Universidad de Chile, Santiago, Chile.

\*Corresponding author(s). E-mail(s): [gonzalo.m@uchile.cl](mailto:gonzalo.m@uchile.cl);

Contributing authors: [pablo.carrasco@pregrado.uoh.cl](mailto:pablo.carrasco@pregrado.uoh.cl);

## Abstract

The non-convex nature of trained neural networks has created significant obstacles in their incorporation into optimization models. Considering the wide array of applications that this embedding has, the optimization and deep learning communities have dedicated significant efforts to the convexification of trained neural networks. Many approaches to date have considered obtaining convex relaxations for each non-linear activation in isolation, which poses limitations in the tightness of the relaxations. Anderson et al. (2020) strengthened these relaxations and provided a framework to obtain the convex hull of the graph of a piecewise linear convex activation composed with an affine function; this effectively convexifies activations such as the ReLU together with the affine transformation that precedes it. In this article, we contribute to this line of work by developing a recursive formula that yields a tight convexification for the composition of an activation with an affine function for a wide scope of activation functions, namely, convex or “S-shaped”. Our approach can be used to efficiently compute separating hyperplanes or determine that none exists in various settings, including non-polyhedral cases. We provide computational experiments to test the empirical benefits of these convex approximations.

**Keywords:** neural networks, convex envelopes, non-convex optimization

# 1 Introduction

Neural networks have seen wide success due to their impressive capabilities in multiple learning tasks. Nowadays, we see neural networks being deployed in many different areas, and we can expect that this trend will continue.

Due to their ubiquity and performance, great efforts are being put into the incorporation of neural networks in optimization models. Some examples of where this embedding has been considered are the generation of adversarial examples [1–3], verification and robustness certification [4–7], feature visualization [2], counting linear regions [8–10], network compression [11–13], neural surrogate models [14, 15], to mention a few. Well-established optimization solvers have recently included modeling capabilities that allow this embedding of trained neural networks, among other modern machine learning models (e.g. [16, 17]). For more examples of the incorporation of trained neural networks in optimization models, we refer the reader to the survey [18].

The main challenge when including a trained neural network in an optimization model is its inherent nonconvexity; this is one of the main sources of expressiveness but, from an optimization standpoint, can pose significant difficulties.

Let us be more specific about where this non-convex behavior comes from. A fully-connected feed-forward neural network is a function, which we denote  $\text{NN}(x)$ , defined as an alternating composition of linear and non-linear functions. They are typically represented as a layered graph: for a network  $G = (V, E)$ , the set of nodes (or neurons) decomposes into  $k$  layers  $\{V_i\}_{i=1}^k$  with  $V = \bigcup_{i=1}^k V_i$ . All nodes in a layer  $V_i$  are connected to all nodes in layer  $V_{i+1}$ , and there are only arcs between adjacent layers. The evaluation of  $\text{NN}(x)$  starts from a given input  $x$  in the first layer. An affine transformation  $W^{(1)\top}x + b^{(1)} =: a^{(2)}$  is computed, where the vector  $a^{(2)}$  has one component per node in  $V_2$ . Each node in  $V_2$  then computes a non-linear activation function  $h_j^{(2)} := \sigma(a_j^{(2)})$  for  $j = 1, \dots, |V_2|$ . Arguably, the most popular activation is the Rectified Linear Unit (ReLU) defined as  $\sigma(x) = \max\{0, x\}$ , but we will discuss some alternatives below. After the activation is computed, the vector  $h^{(2)}$  is considered as the input of a new affine function  $W^{(2)\top}h^{(2)} + b^{(2)} =: a^{(3)}$  and the process is then iterated until the last layer is reached. In some cases, in the last layer, an extra transformation is applied; however, this will be out of the scope of this paper, so we will omit it from our discussion. The nonconvexity of the neural network can be traced to the presence of the activation function: these are non-linear functions, and even when they are convex, their alternating composition with linear functions yields non-convex behaviors.

When expressing the neural network evaluation within an optimization model, a typical approach is to follow the same nested composition of functions, define the vectors  $h^{(i)}, a^{(i)}$ , for  $i = 1, \dots, k$ , as variables, and impose the following constraints

$$h^{(1)} = x \tag{1a}$$

$$W^{(i)\top}h^{(i)} + b^{(i)} = a^{(i+1)} \quad \forall i = 1, \dots, k \tag{1b}$$

$$h^{(i)} = \sigma(a^{(i)}) \quad \forall i = 2, \dots, k \tag{1c}$$

where the activation function is applied component-wise. In this case, the non-convexity has been isolated to the equations  $h^{(i)} = \sigma(a^{(i)})$  which, even when  $\sigma$  is convex, are non-convex constraints.

To convexify such a system, one can construct a convex relaxation of each of the equations of the form  $y = \sigma(z)$ , which in turn yields an extended formulation of a convex relaxation of  $\{(x, y) : y = \text{NN}(x)\}$ . In these lines, much work has been focused on constructing convex relaxations of  $\{(z, y) : y = \sigma(z)\}$ . We refer the reader to [6] for various convexifications that have been used in the ReLU case. Beyond the ReLU case, researchers have also focused on leveraging the concave and convex envelopes of  $\sigma$  when neural networks are embedded in optimization models [19, 20]. We also discuss other convexification approaches below.

One of the limitations of the aforementioned techniques is that they consider each activation function separately, i.e., they convexify a set of the form  $\{(z, y) \in D \times \mathbb{R} : y = \sigma(z)\}$ , where  $D$  is an interval, and do not take into account that the input  $z$  is an affine transformation of a vector, or that the inputs of different neurons on a layer are related. This is the so-called “single neuron convex barrier” [21]. We highlight two different high-level paths that have tackled this barrier. The first type of approach has focused on convexifying multiple activation functions of a single layer simultaneously, leveraging that their inputs are related. Broadly speaking, these approaches consider groups of constraints of the type (1c) and, starting from polyhedral constraints on the  $a$  variables, they construct relational constraints that involve groups of  $h$  variables. See e.g. [22–27]. We also refer the reader to [28] for a survey. In these approaches, obtaining convex hulls is usually intractable, and thus the authors strive for efficiency by relying on tractable polyhedra for the  $a$  variables, and not considering all neurons of a layer simultaneously.

The second type of approach we identify is that of [29], who presented a method for obtaining the convex hull of  $\{(x, y) \in D \times \mathbb{R} : y = \sigma(w^\top x + b)\}$  where  $D$  is a polyhedron and  $\sigma$  is a piecewise linear convex function (e.g. the ReLU activation). This considers one activation function, but it combines it with the output of all neurons of the previous layer. The authors propose an elaborate framework to produce a description of the convex hull of the set along with an efficient separation routine.

Both of these approaches break the single-neuron convex barrier, but there are trade-offs in both. In one case, multiple activations are convexified simultaneously, but only relaxations are obtained. In the other case, a convex hull can be obtained, along with an efficient separation routine, but considers one activation function.

## 1.1 Contribution

In this paper, we follow the line of [29] and consider the convexification of  $\{(x, y) \in D \times \mathbb{R} : y = \sigma(w^\top x + b)\}$  when  $D \subseteq \mathbb{R}^n$  is a box domain and  $\sigma$  is a convex or an “S-shaped” activation (properly defined below). For this family, we obtain a recursive formula that yields the convex hull

$$\text{conv}(\{(x, y) \in D \times \mathbb{R} : y = \sigma(w^\top x + b)\}).$$

The main ingredient is the computation of the convex and concave envelope of the function  $f(x) = \sigma(w^\top x + b)$  over a box domain. Our recursive description provides a unified perspective for a wide variety of activation functions that can be used to determine if a given  $(x, y) \in \text{conv}(\{(x, y) \in D \times \mathbb{R} : y = \sigma(w^\top x + b)\})$  using at most  $n$  simple one-dimensional convexifications. It also allows us to efficiently construct a separating hyperplane if one exists.

To evaluate the impact of the convex hull description, we provide multiple computational experiments. Mainly, we evaluate the use of our convex hull description through a cutting plane method when computing so-called *activation bounds*, that is, computing bounds on the variables  $a^{(i)}$ , which are typically used for improving convex estimates of the non-convex expressions within the evaluation of  $\text{NN}(x)$ .

To the best of our knowledge, no work has provided a method for computing  $\text{conv}(\{(x, y) \in D \times \mathbb{R} : y = \sigma(w^\top x + b)\})$  beyond piecewise-linear convex activations.

## 1.2 Outline

This paper is organized as follows. In Section 2, we review relevant literature from both the neural network and the convex envelope perspectives. In Section 3, we state our main result formally and discuss its reach. In Section 4, we provide all the preliminary technical results, which are then used in Section 5 for the proof of our main result. In Section 6, we show computational experiments showing the potential of using the envelopes we develop here. Finally, in Section 7, we conclude.

## 1.3 Notation

We denote  $\mathbb{R}_+^n$  the set of vectors where *all* their entries are *strictly positive*. We denote as  $e_i \in \mathbb{R}^n$  the  $i$ -th canonical vector and  $\mathbf{1}$  the vector of all ones. For  $x \in \mathbb{R}^n$ , we denote  $x_{-i}$  the  $(n - 1)$ -dimensional vector given by all entries except  $x_i$ , i.e.,  $x_{-i} = (x_1, \dots, x_{i-1}, x_{i+1}, \dots, x_n)$ . For a function  $f : [0, 1]^n \rightarrow \mathbb{R}$  we denote  $f_{-i} : [0, 1]^{n-1} \rightarrow \mathbb{R}$  the function obtained by restricting  $f$  to have the  $i$ -th input to 1. To avoid ambiguity, we always write the argument of  $f_{-i}$  as  $x_{-i}$ , thus:

$$f_{-i}(x_{-i}) = f(x_1, \dots, x_{i-1}, 1, x_{i+1}, \dots, x_n).$$

For a set  $S \subseteq \mathbb{R}^n$ , we denote  $\text{int}(S)$ ,  $\text{cl}(S)$  and  $\text{conv}(S)$  its interior, closure and convex hull, respectively. For a function  $f$ , we denote  $\text{conc}(f, S)$  its concave envelope over  $S$ . This is the smallest concave function that upper bounds  $f$  on the domain  $S$ . Similarly, we denote  $\text{conv}(f, S)$  its convex envelope over  $S$ .

## 2 Literature review

Our work touches on two major research areas: the convex approximations of trained neural networks and function envelope computations.

### *Approximation of trained neural networks*

Many efforts in convexifying a trained neural network have focused on convexifying equations of the form  $y = \sigma(z)$ . When  $\sigma(z) = \max\{0, z\}$  (i.e., in the ReLU case),

the convex hull of  $\{(z, y) : y = \sigma(z)\}$  has been used in multiple optimization tasks, e.g., in neural network verification [6]. Beyond the ReLU case, the concave and convex envelopes of activations functions have been used successfully in the incorporation of neural networks in deterministic optimization models [19, 20]. Also see [30].

As mentioned in the introduction, one of the limitations of the aforementioned approaches is that they consider each activation function separately [21]. Specifically, when building a convex relaxation, they convexify sets of the form  $\{(z, y) : y = \sigma(z)\}$  without considering the preceding affine transformation that feeds the activation or the relations between different neurons of the same layer through their inputs. In [29], for example, the authors note that the relaxation of the popular big-M mixed-integer formulation of the ReLU function yields the best possible relaxation for a single neuron, but this is no longer true when the same formulation is used for representing  $y = \sigma(w^\top x + b)$ .

In [22], the authors take a step towards breaking this barrier and propose a method for convexifying multiple ReLU neurons simultaneously. Their approach is able to produce convex relaxations that consider relational constraints (i.e., constraints beyond individual intervals) on groups of activations of the same layer. Subsequent works have further elaborated and expanded this type of approach [23–27]. We also refer the reader to the survey [28].

A different path to tackle the single neuron convex barrier was taken in [29], where the authors consider a single activation along with the preceding affine function. Specifically, they construct an *ideal formulation*<sup>1</sup> for  $\{(x, y) \in D \times \mathbb{R} : y = \sigma(w^\top x + b)\}$ , where  $D$  is a polytope, that uses only one binary variable; this can be used to obtain the convex hull of the set. To do this, the authors study the more general set  $\{(x, y) \in D \times \mathbb{R} : y = f(x)\}$  where  $f$  is a piecewise linear convex function. While these results provide strong relaxations, their practical performance can be worse than the weaker big-M formulation. To remedy this, in [31–33], the authors show strategies for obtaining intermediate formulations, i.e., formulations that can capture the strength of the convex hull formulation and the empirical efficiency of the big-M formulations.

Other approaches to handle the non-convexities of a trained neural network include using convex *restrictions* [34], piecewise-linear approximations of smooth activations [35], piecewise-linear *relaxations* of activation functions [36], lagrangian relaxations [37], semidefinite relaxations [38], and convexifications of the softmax function [39]. For a unified perspective on convex relaxations in verification contexts for the ReLU networks, see [21].

To the best of our knowledge, besides [29], none of these works have provided a method for obtaining  $\text{conv}(\{(x, y) \in D \times \mathbb{R} : y = \sigma(w^\top x + b)\})$ .

### *Convex and concave envelopes*

The optimization community has produced a wide spectrum of alternatives in envelope computations. A commonly used envelope is that of the bilinear function  $f(x_1, x_2) = x_1 x_2$  over a rectangular region, for which the convex (and concave) envelope is obtained through the so-called McCormick envelopes [40, 41].

---

<sup>1</sup>An ideal formulation is a mixed-integer extended formulation such that its continuous relaxation is tight, and that also satisfies an extra integrality property. See [29].

One important stream of works has focused on the polyhedral case, i.e., when the function has a polyhedral envelope. In [42, 43], for example, it is shown that *edge-concavity* of a function  $f$  (i.e., concavity over all edge directions of a polytope  $P$ ) implies that the convex envelope of  $f$  over  $P$  is polyhedral. The construction of these convex envelopes is studied in [44]. The convex envelope of multilinear functions is considered in [45–47]. In [48], the authors study the facets of the convex envelope of a trilinear monomial over a box. In [49], the authors propose a cutting plane approach to obtain the convex envelope of a bilinear function over a box. The strength of the convex underestimator of a bilinear function that is obtained from using term-wise convex envelopes is analyzed in [50]. In [51], the authors derive explicit convex and concave envelopes of several functions on sub-sets of a hyper-rectangle, which are obtained through polyhedral subdivisions. In this case, the authors can obtain, in closed form, the convex envelope of disjunctive functions of the form  $xf(y)$  and the concave envelope of *concave-extendable* supermodular functions.

Computing envelopes in dimension at most two has also been an active research area. In [52], the authors tackle the bilinear bivariate functions over a class of special polytopes called  $D$ -polytopes. The envelope of a fractional function  $x_1/x_2$  has been studied over a rectangle [53, 54] and over a trapezoid [55]. This was expanded in [56], where convex envelopes for bilinear and fractional bivariate functions over quadrilaterals are constructed. Bilinear bivariate functions over a triangle have been considered in [52, 57, 58]. A closed-form expression for the convex envelope of  $x_1x_2$  over a box intersected with a halfspace was obtained in [59]. Bivariate functions over arbitrary polytopes are considered in [60–63]. Cubic functions in two dimensions were considered in [64], and odd-degree monomials over an interval in [65]. A general discussion on envelopes for univariate functions can be found in [66].

Since our setting yields non-polyhedral envelopes in arbitrary dimensions, the settings of the two previous paragraphs do not directly apply to our case.

Multiple works have handled functions that may have non-polyhedral envelopes in arbitrary dimensions. In [54], the authors develop a disjunctive programming approach to obtain the convex envelope for functions that are concave on one variable, convex on the rest, and defined over a rectangular region. In [67], the authors study convex extensions of functions and provide conditions under which the tightest convex extension is the convex envelope. Later on, in [68], the authors show how to compute the evaluation of  $\text{conc}(f, R)$  when  $f$  is an  $(n-1)$ -convex function (i.e.,  $f$  is convex whenever one variable is fixed to any value) and  $R$  is a rectangular domain. In [69, 70], the authors formulate the convex envelope of a lower semi-continuous function over a compact set as a convex optimization problem. They use this to compute, explicitly, the convex envelope for various functions that are the product of a convex function and a component-wise concave function over a box. In [71], the authors show how to compute the convex envelope of a function that is concave on the rays emanating from the origin and is convex on the facets of a polytope.

To the best of our knowledge, most of the approaches of the last paragraph do not apply to functions of the type  $\sigma(w^\top x + b)$ , where  $\sigma$  is neither concave nor convex. The only exception in terms of applicability is the convex optimization formulation for the envelope computation considered in [69, 70], which is very general. However, it

is unclear to us how to exploit this formulation in order to obtain a simple expression of the envelope.

### 3 Main result and discussion

#### 3.1 Set-up

As mentioned in the introduction, we are interested in computing

$$\text{conv}(\{(x, y) \in D \times \mathbb{R} : y = \sigma(w^\top x + b)\}),$$

where  $\sigma : \mathbb{R} \rightarrow \mathbb{R}$ ,  $w \in \mathbb{R}^n$ ,  $b \in \mathbb{R}$ , and  $D$  is a bounded box domain. Let  $f(x) = \sigma(w^\top x + b)$ . We assume throughout that  $\sigma$  is continuous, which ensures that the epigraph and hypograph of  $f$  are closed sets and that the previous convex hull of the graph is a closed set as well.

In this setting,

$$\begin{aligned} & \text{conv}(\{(x, y) \in D \times \mathbb{R} : y = f(x)\}) \\ &= \{(x, y) \in D \times \mathbb{R} : \text{conv}(f, D) \leq y \leq \text{conc}(f, D)\} \end{aligned}$$

i.e., computing the convex hull of the graph of  $f$  can be reduced to computing the convex and concave envelope of  $f$ . In this paper, we focus on computing  $\text{conc}(f, D)$  for  $\sigma$  functions that are either convex or S-shaped. In terms of the convex envelope, when  $\sigma$  is convex, then  $\text{conv}(f, D) = f$ , and when  $\sigma$  is S-shaped, we will show that the concave envelope “recipe” can also be used for the convex envelope computation.

Before continuing, let us specify what we mean by S-shaped.

**Definition 1.** *We say a continuous function  $\sigma : \mathbb{R} \rightarrow \mathbb{R}$  is S-shaped, if there exists  $\tilde{z}$  such that  $\sigma : (-\infty, \tilde{z}] \rightarrow \mathbb{R}$  is a convex function and  $\sigma : [\tilde{z}, \infty) \rightarrow \mathbb{R}$  is a concave function.*

**Remark 1.** *The reader may notice that our definition of S-shaped is very similar to well-known families of functions. However, there are some subtle differences.*

- *The class of differentiable S-shaped functions is commonly known as sigmoid functions. In [20, 72], the authors use the term convexo-concave for them. In our case, it will be important not to assume differentiability to include more activation functions, which is why we chose not to use either of these names.*
- *Additionally, in the deep learning literature, the term sigmoid is commonly reserved for the logistic function  $1/(1 + e^{-x})$ . This is another reason why we opted for an alternative name.*

To unify our discussion, we define the following property that both convex and S-shaped functions satisfy.

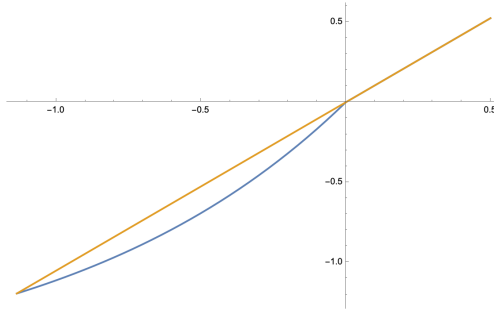


**Fig. 1:** Plot of the SELU activation (blue) overlapped with its concave envelope (orange) in the interval  $[-1.13, 0.5]$ . See Table 2 for the definition of this activation. In this interval, the concave envelope is a linear function, which is equal to  $\sigma(x)$  for every  $x \geq 0$ ; therefore there are multiple  $\hat{z}$  for accommodating property (2). According to our definition, the tie point would be unambiguously defined as 0.

**Definition 2.** We say the continuous function  $\sigma : \mathbb{R} \rightarrow \mathbb{R}$  satisfies the secant-then-function envelope (STFE) property if

$$\forall [\ell, u] \subseteq \mathbb{R}, \exists \hat{z} \in [\ell, u], \text{conc}(\sigma, [\ell, u])(z) = \begin{cases} \sigma(\ell) + \frac{\sigma(\hat{z}) - \sigma(\ell)}{\hat{z} - \ell}(z - \ell) & \text{if } z \in [\ell, \hat{z}] \\ \sigma(z) & \text{if } z \in [\hat{z}, u] \end{cases} \quad (2)$$

that is, as the name suggests, the concave envelope of  $\sigma$  on any interval is given by a secant to  $\hat{z}$ , and then the function itself.

For a given  $[\ell, u]$ , we call the smallest point  $\hat{z}$  satisfying (2) the tie point of  $\sigma$  over  $[\ell, u]$ .

**Remark 2.**

- It is not hard to see that if  $\sigma$  is either convex, concave, or S-shaped, then the STFE property is satisfied. For a convex or concave case, it is direct. For the differentiable S-shaped case, it was already exploited by [20], and similar arguments can be found in [65, 66]. We have not found an argument handling the non-differentiable case, but using a result from [67], it follows directly (see Appendix A).

We believe that the STFE property is actually equivalent to the function being in one of these three categories (convex, concave, or S-shaped), but we have not yet found a proof.

- We are borrowing the name “tie point” from the case when  $\sigma$  is S-shaped and differentiable: in this case,  $\hat{z}$  is computed as a point where the secant slope in  $[\ell, \hat{z}]$  equals the derivative of  $\sigma$  on  $\hat{z}$  [20, 66, 72]. In our definition, this “tie” may not happen (e.g., in a strictly convex case), or multiple points may satisfy it (see Figure 1), which is why we take the smallest one.



Recall that we are considering  $f : D \subseteq \mathbb{R}^n \rightarrow \mathbb{R}$  defined as  $f(x) = \sigma(w^\top x + b)$  where  $D$  is a bounded box domain. Note that we can simplify the setting the following way without loss of generality:

1. We can assume  $w_i > 0$ , for all  $i = 1, \dots, n$ , by reducing the dimension when  $w_i = 0$  and changing variables  $x_i \rightarrow -x_i$  when  $w_i < 0$ .
2. After the previous modifications, we can rescale and shift the variables to get  $x \in [0, 1]^n$ . This changes  $w$  and  $b$  but does not change the sign of  $w$ .

One can easily verify that computing the concave envelope of the modified setting is equivalent to the original one.

### 3.2 Main result

Our main result is a recursive formula for the concave envelope of a function  $f : [0, 1]^n \rightarrow \mathbb{R}$  of the form  $f(x) = \sigma(w^\top x + b)$  where  $w > 0$  and  $\sigma$  satisfies the STFE property. Our recursive formula is based on the fact that if we fix, say,  $x_i = 1$ , then

$$f_{-i}(x_{-i}) = \sigma(w_{-i}^\top x_{-i} + (b + w_i))$$

also has the desired structure. Our concave envelope construction is based on a polyhedral subdivision of the domain and taking secants of  $f$  on rays emanating from the origin in some of the regions. This is akin to the constructions in [51, 71]; however, these settings do not apply here, and thus, we need a new proof.

For the construction, we define the following subdivision of  $[0, 1]^n$ .

**Definition 3.** Given  $w \in \mathbb{R}_+^n$ ,  $b \in \mathbb{R}$ , and  $\hat{z} \in \mathbb{R}$ , we define

$$\begin{aligned} R_f &:= \{x \in [0, 1]^n : w^\top x + b \geq \hat{z}\} \\ R_l &:= \{x \in [0, 1]^n : w^\top x + b < \hat{z}, w^\top x + b \|x\|_\infty \geq \hat{z} \|x\|_\infty\} \\ R_i &:= \{x \in [0, 1]^n : w^\top x + b \|x\|_\infty < \hat{z} \|x\|_\infty, \\ &\quad x_i > x_j \quad \forall j < i, x_i \geq x_j \quad \forall j \geq i\} \quad i = 1, \dots, n \end{aligned}$$

We will provide some intuition on the meaning of these regions after the main theorem statement, which follows.

**Theorem 1.** Consider  $w \in \mathbb{R}_+^n$ ,  $b \in \mathbb{R}$  and let  $f : [0, 1]^n \rightarrow \mathbb{R}$  be a function of the form  $f(x) = \sigma(w^\top x + b)$  where  $\sigma$  satisfies the STFE property. Then,

$$\text{conc}(f, [0, 1]^n)(x) = \begin{cases} f(x) & \text{if } x \in R_f \\ \sigma(b) + \frac{\sigma(\hat{z}) - \sigma(b)}{\hat{z} - b} (w^\top x) & \text{if } x \in R_l \\ \sigma(b) + x_i \text{conc}(f_{-i} - \sigma(b), [0, 1]^{n-1}) \left( \frac{x_{-i}}{x_i} \right) & \text{if } x \in R_i, i = 1, \dots, n \end{cases}$$

where  $R_f, R_l$  and  $R_i$  are defined using Definition 3 with  $\hat{z}$  as the tie point of  $\sigma$  in  $[b, w^\top \mathbf{1} + b]$ .

Firstly, we note that the sub-indices in the name in the regions make reference to the fact that the envelope is equal to  $f$  in  $R_f$ , *linear* in  $R_l$ , and that the  $i$ -th component of  $x$  is the largest in  $R_i$ . We heavily use these names below, so we hope this can help the reader remember their meanings.

We also remark that some regions may be empty or low-dimensional. In addition, they are disjoint, and thus, there is no ambiguity:  $R_f \cap R_l = \emptyset$  and  $R_i \cap R_l = \emptyset$  can be directly verified. The case  $R_i \cap R_j = \emptyset$  for  $i \neq j$  can also be checked easily. As for  $R_i \cap R_f$ , one can use that for  $x \in [0, 1]^n \setminus \{0\}$  and  $w > 0$  we have  $w^\top x \leq w^\top x / \|x\|_\infty$  to show that  $R_i \subseteq \{x : w^\top x + b < \hat{z}\}$ . Note that one can also easily see that they partition  $[0, 1]^n$ . Moreover, the main reason behind  $R_i$  to have strict and non-strict inequalities is for achieving this partition; this is not really crucial since we will mainly work with their interiors, in which case for  $x \in \text{int}(R_i)$  we have  $x_i > x_j$  for all  $j \neq i$ .

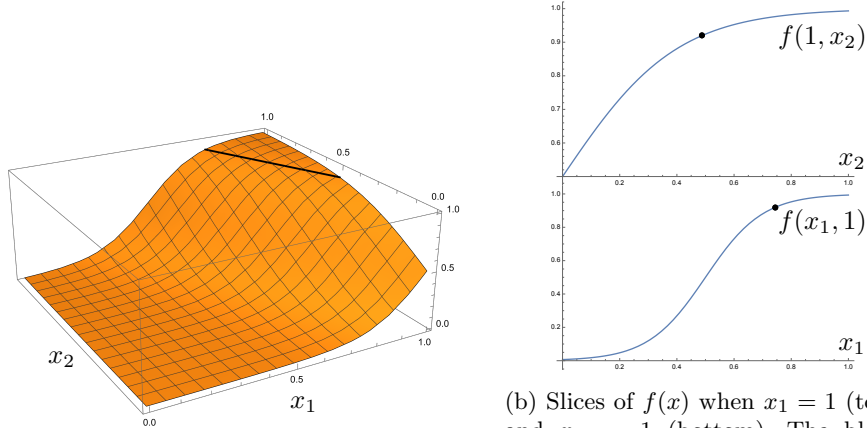
The power of Theorem 1 is that it gives us a direct way of evaluating  $\text{conc}(f, [0, 1]^n)(x)$  for a given  $x$ : this is either a direct function evaluation in  $R_l$  or  $R_f$ , or an envelope evaluation in one lower dimension. Since we require the computation of a tie point for the construction of the regions, in the worst case, we need to compute a one-dimensional concave envelope of  $\sigma$  for  $n$  different intervals. One could also derive a full, explicit (i.e., non-recursive) description of the envelope for variable  $x$  from Theorem 1. However, this may involve exponentially many region combinations, as opposed to the  $n$  evaluations needed for a fixed  $x$ .

Theorem 1 is also useful for computing gradients of the concave envelope on a given  $x$ , almost everywhere. If  $x \in R_f \cup R_l$ , the gradient computation is direct. If  $x \in R_i$  for some  $i$ , assuming  $\text{conc}(f_{-i}, [0, 1]^{n-1})$  is differentiable at  $x_{-i}/x_i$  we can compute the gradient simply using the chain rule: let  $g_{ave} = \text{conc}(f, [0, 1]^n)$  and  $g_{ave,-i} = \text{conc}(f_{-i}, [0, 1]^{n-1})$ , then,

$$\begin{aligned} \frac{\partial}{\partial x_j} g_{ave}(x) &= \frac{\partial}{\partial x_j} g_{ave,-i}(x_{-i}/x_i) & j \neq i \\ \frac{\partial}{\partial x_i} g_{ave}(x) &= g_{ave,-i}(x_{-i}/x_i) - \sigma(b) - \nabla g_{ave,-i}(x_{-i}/x_i)^\top \begin{pmatrix} x_{-i} \\ x_i \end{pmatrix}. \end{aligned}$$

We remind the reader that  $x_{-i}$  and the domain of  $g_{ave,-i}$  are  $(n-1)$ -dimensional, and thus the last inner product is between two  $(n-1)$ -dimensional vectors.

This can be useful when an approximation of the envelope is computed on the fly, as in a cutting plane fashion. If we have  $(\hat{x}, \hat{y})$  such that  $\text{conc}(f, [0, 1]^n)(\hat{x}) < \hat{y}$ , we can construct a separating hyperplane, using at most  $n$  gradient computations.



(a) Plot of  $f(x)$  over the hypercube (orange) and line given by  $w^\top x + b = \hat{z}$  (black).

(b) Slices of  $f(x)$  when  $x_1 = 1$  (top) and  $x_2 = 1$  (bottom). The black points are the intersection of the line  $w^\top x + b = \hat{z}$  and each slice.

**Fig. 2:** Plots of the function  $f(x) = \sigma(w^\top x + b)$  defined with the parameters of Example 1, along with the slices given by setting the variables to 1.

**Example 1.** Throughout this paper, we will use the following running example to illustrate our construction and proof ideas. We consider the sigmoid activation

$$\sigma(x) = \frac{1}{1 + e^x}$$

$w = (10, 5)$ , and  $b = -10$ . In Figure 2 we show a plot of the function, and of the slices given by  $x_1 = 1$  and  $x_2 = 1$ , which are used in the envelope computation.

We display the envelope described in Theorem 1 in Figure 3. We note a few important facts to motivate our construction. Firstly, note that the concave envelopes that are computed recursively will not be affine in general. This can be observed in both regions  $R_1$  (red) and  $R_2$  (purple) and on their slices shown in Figure 3(b).

Additionally, the tie point used to compute the envelope in both facets does not lie on the line  $w^\top x + b = \hat{z}$ , where  $\hat{z}$  is the tie point of  $\sigma$  in  $[b, w^\top \mathbf{1} + b]$ . This is because, in each facet, the argument of  $\sigma$  has a different range. However, note that in both cases, the tie point on the slice is “on the left” of the points that are determined by  $\hat{z}$ . This is not a coincidence, and we will prove below that this always happens. This is also related to [67, Corollary 2], which states that the concave envelope restricted to a face coincides with the envelope computed on the face.

### 3.3 Reach of this framework

Before moving to the proofs, we describe the reach of our tools in the trained neural network setting. While the STFE property may seem restrictive, a large portion of the most commonly used activation functions satisfies this property: as mentioned

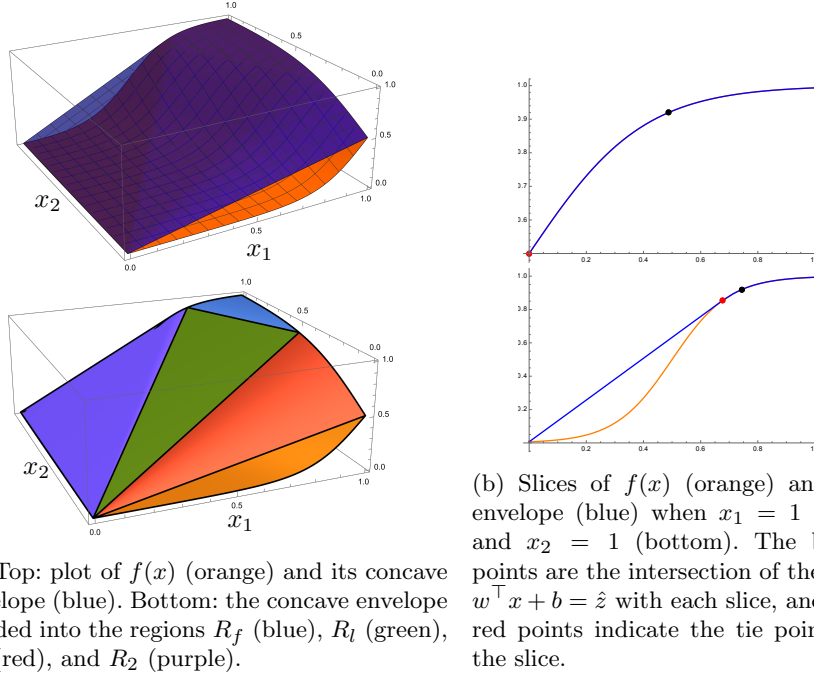


**Fig. 3:** Plots of the concave envelope of the function  $f(x) = \sigma(w^\top x + b)$  defined with the parameters of Example 1, along with the slices given by setting the variables to 1.

earlier, all convex and S-shaped activations satisfy it, which was already exploited for differentiable S-shaped activations in [20].

### 3.3.1 Concave envelopes for convex activations

The first major family where our framework can be applied is given by convex activation functions. In Table 1, we provide a list of common convex activations.

Our results provide an alternative perspective on the envelopes developed in [29] when the domain is a box. One notable difference is that, for the ReLU case on a box domain, the authors in [29] provide an explicit formula of exponential size for the convex hull, while we provide a non-explicit recursive formula. In both cases, however, an efficient separation algorithm exists. We also remark that our approach is limited to box domains, which is not the case for the general framework in [29].

Since these functions are convex, their convex envelope is the function itself; therefore, we only need the concave envelope in order to recover the convex hull of the graph of  $f$ .

### 3.3.2 Concave and convex envelopes for S-shaped activations

Another important family of activations we can consider with our framework is the S-shaped functions. In Table 2, we provide a list of common S-shaped activations,

**Table 1:** List of common convex activation functions

Name	Parameters	Function $\sigma(x)$
Rectifier Linear Unit (ReLU)		$\max\{0, x\}$
Leaky ReLU	$0 < \varepsilon < 1$	$\begin{cases} x, & \text{if } x > 0 \\ \varepsilon x, & \text{if } x \leq 0 \end{cases}$
Maxtanh		$\max\{x, \tanh(x)\}$
Softplus		$\log(1 + \exp(x))$
Exponential Linear Unit (ELU)	$0 < \alpha \leq 1$	$\begin{cases} x, & x > 0 \\ \alpha(\exp(x) - 1), & x \leq 0 \end{cases}$

**Table 2:** List of common S-shaped activation functions

Name	Parameters	Function $\sigma(x)$
Softsign		$\frac{x}{1 +  x }$
Hyperbolic tangent		$\tanh(x)$
Penalized hyperbolic tangent	$0 < \alpha < 1$	$\begin{cases} \tanh(x), & x > 0 \\ \tanh(\alpha x), & x \leq 0 \end{cases}$
Sigmoid		$\frac{1}{1 + \exp(-x)}$
Bipolar sigmoid		$\frac{1 - \exp(-x)}{1 + \exp(-x)}$
Exponential Linear Unit (ELU)	$\alpha > 1$	$\begin{cases} x, & x > 0 \\ \alpha(\exp(x) - 1), & x \leq 0 \end{cases}$
Scaled Exponential Linear Unit (SELU)	$\lambda = 1.0507$ $\alpha = 1.67326$	$\lambda \begin{cases} x, & x > 0 \\ \alpha(\exp(x) - 1), & x \leq 0 \end{cases}$
Sigmoid Linear Unit (SiLU)		$\frac{x}{1 + \exp(-x)}$

some of which are not differentiable everywhere. We note that the SiLU activation function is not technically S-shaped since it is concave *and then* convex. However, we can simply reflect the domain to obtain an S-shaped function, compute the envelope, and then reflect again.

While our recipe yields concave envelopes, in the case of S-shaped functions, we can also obtain convex envelopes. This can be seen by noting that if  $\sigma$  is S-shaped, then  $\sigma'(z) = -\sigma(-z)$  is also S-shaped, and computing the concave envelope  $\sigma'(w^\top y - b)$  yields the convex envelope of  $\sigma(w^\top x + b)$  using the change of variables  $y = -x$ .

## 4 Preliminary results

### 4.1 One-dimensional properties

In this section, we collect a number of simple properties for a  $\sigma$  function that satisfies STFE. Since these properties are rather intuitive, we relegate their proofs to Appendix B. However, we note that they are not direct, as we assume having information on the envelope of the function but not directly on the function itself. We remind the reader

that the STFE property states that the envelope is given by a secant and then the function for *every* interval.

**Lemma 2.** *Let  $\sigma : \mathbb{R} \rightarrow \mathbb{R}$  be a function satisfying STFE, with a tie point  $\hat{z}$  on an interval  $[L, U]$ . Then the following properties hold:*

1. **(Decreasing upper bound, case 1)** *For every  $\tilde{U} \in [\hat{z}, U]$ ,*

$$\text{conc}(\sigma, [L, \tilde{U}])(z) = \text{conc}(\sigma, [L, U])(z) \quad \forall z \in [L, \tilde{U}]$$

*and  $\hat{z}$  is the tie point of  $\sigma$  in the interval  $[L, \tilde{U}]$  as well.*

2. **(Decreasing upper bound, case 2)** *For every  $\tilde{U} \in [L, \hat{z}]$ ,*

$$\text{conc}(\sigma, [L, \tilde{U}])(z) = \sigma(L) + \frac{\sigma(\tilde{U}) - \sigma(L)}{\tilde{U} - L}(z - L).$$

3. **(Increasing lower bound)** *For any  $\tilde{L} \in [L, \hat{z}]$  let  $\tilde{z}$  be the tie point of  $\sigma$  in  $[\tilde{L}, U]$ . Then  $\tilde{z} \leq \hat{z}$ .*

There is a subtle point in Case 2 of the previous lemma. Take, for instance  $\sigma(z) = \max\{0, z\}$  the ReLU activation. The tie point in an interval  $[-1, \varepsilon]$  for  $\varepsilon > 0$  is  $\varepsilon$ . However, for  $[-1, 0]$ , the tie point is  $-1$ : the tie point “jumps” when moving the upper bound after a certain threshold. This is because  $\sigma$  is linear in  $[-1, 0]$ , and our definition of the tie point is a minimum. For this reason, in Case 2, we did not specify the tie point. One could think of redefining the tie point as a maximum, but this brings other technical issues.

## 4.2 General properties of the envelope

We begin by stating a result from [67] (slightly rephrased), which we will repeatedly use.

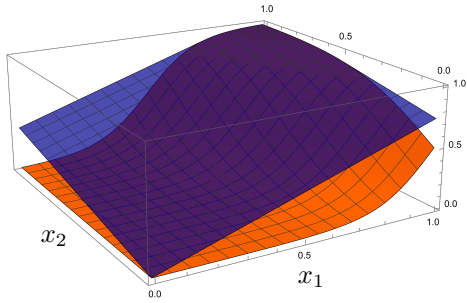
**Lemma 3.** [67, Corollary 2] *Let  $D$  be a convex set and  $D'$  be a non-empty face of  $D$ . Assume  $\phi(x)$  is the concave envelope of  $f(x)$  over  $D$ . Then, the restriction of  $\phi(x)$  to  $D'$  is the concave envelope of  $f(x)$  over  $D'$ .*

The following defines a “baseline” concave overestimator for  $f$ .

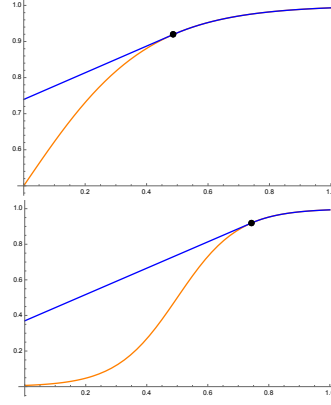
**Lemma 4.** *Consider  $w \in \mathbb{R}_+^n$ ,  $b \in \mathbb{R}$  and let  $f : [0, 1]^n \rightarrow \mathbb{R}$  be a function of the form  $f(x) = \sigma(w^\top x + b)$  where  $\sigma$  satisfies the STFE property. Define  $h : [0, 1]^n \rightarrow \mathbb{R}$  as*

$$h(x) = \begin{cases} f(x) & \text{if } x \in R_f \\ \sigma(b) + \frac{\sigma(\hat{z}) - \sigma(b)}{\hat{z} - b}(w^\top x) & \text{otherwise} \end{cases}$$

*where  $R_f$  is defined using Definition 3 with  $\hat{z}$  as the tie point of  $\sigma$  in  $[b, w^\top \mathbf{1} + b]$ . Then  $h$  is a concave overestimator of  $f$ .*



(a) Plot of  $f(x)$  over the hypercube (orange) and the overestimator  $h(x)$  (blue).



(b) Slices of  $h(x)$  when  $x_1 = 1$  (top) and  $x_2 = 1$  (bottom). The black points are the intersection of the line  $w^\top x + b = \hat{z}$  and each slice.

**Fig. 4:** Plots of the function  $f(x) = \sigma(w^\top x + b)$  defined with the parameters of Example 1, the concave overestimator  $h(x)$  given in Lemma 4, and the slices given by setting the variables to 1.

*Proof.* This proof follows directly since  $h = \text{conc}(\sigma, [b, w^\top \mathbf{1} + b])(w^\top x + b)$ .  $\square$

We note that the  $h$  overestimator can also be viewed through the McCormick estimator “recipe” for the composition of functions [40].

In Figure 4, we plot the function  $h$  defined in Lemma 4, along with the slices given by  $x_1 = 1$  and  $x_2 = 1$ . The reader can compare with Figure 3 to note the difference in the quality of the approximation given by  $h$  and by the concave envelope, especially on the slices.

While the  $h$  overestimator of Lemma 4 may not be equal to the concave envelope, in general, it is not hard to see that in some of the regions, it is.

**Lemma 5.** Consider  $h : [0, 1]^n \rightarrow \mathbb{R}$  as in Lemma 4 and the regions defined in Definition 3. For any  $x \in R_f \cup R_l$ ,  $h(x) = \text{conc}(f, [0, 1]^n)(x)$ .

*Proof.* If  $x \in R_f$ , then the result is trivial. If  $x \in R_l$  and  $x = 0$ , then the result is also trivial since  $h(0) = \sigma(b) = f(0)$ . Finally, we consider  $x \in R_l \setminus \{0\}$ , then, we can take  $\lambda > 1$  such that

$$w^\top(\lambda x) + b = \hat{z}$$

Since  $x \in R_l$ ,  $\lambda \leq 1/\|x\|_\infty$  and thus  $\lambda x \in [0, 1]^n$ ; moreover  $\lambda x \in \text{cl}(R_l) \cap R_f$ . With this,

$$h(x) = \frac{1}{\lambda} h(\lambda x) + \left(1 - \frac{1}{\lambda}\right) h(0) \quad (h \text{ affine})$$

$$\begin{aligned}
&= \frac{1}{\lambda} f(\lambda x) + \left(1 - \frac{1}{\lambda}\right) f(0) && (h = f \text{ in } R_f \cup \{0\}) \\
&\leq \frac{1}{\lambda} \text{conc}(f, [0, 1]^n)(\lambda x) + \left(1 - \frac{1}{\lambda}\right) \text{conc}(f, [0, 1]^n)(0) \\
&\leq \text{conc}(f, [0, 1]^n)(x).
\end{aligned}$$

Since  $h$  is a concave overestimator, we conclude.  $\square$

Additionally, we have the following consequence of Lemma 5.

**Lemma 6.** *Let  $\hat{z}$  be the tie point of  $\sigma$  in  $[b, w^\top \mathbf{1} + b]$ . For every  $z \geq \hat{z}$ ,*

$$\text{conc}(f, [0, 1]^n)(x) = \text{conc}(f, [0, 1]^n \cap \{x : w^\top x + b \leq z\})(x)$$

for every  $x$  such that  $w^\top x + b \leq z$ .

*Proof.* The function  $\text{conc}(f, [0, 1]^n \cap \{x : w^\top x + b \leq z\})$  can only be smaller since it's an envelope over a reduced domain. Following the same proof as in Lemma 5, one can show that

$$\text{conc}(f, [0, 1]^n \cap \{x : w^\top x + b \leq z\})(x) = f(x)$$

for every  $x$  such that  $w^\top x + b \in [\hat{z}, z]$ , thus, we can extend  $\text{conc}(f, [0, 1]^n \cap \{x : w^\top x + b \leq z\})$  to  $[0, 1]^n$  simply using  $f$ ; this will yield a concave function which must be  $\text{conc}(f, [0, 1]^n)$ .  $\square$

There is one important detail in our formula for the concave envelope of  $f$  in Theorem 1: in the region  $R_i$ , the lower dimensional envelope is computed in the whole face given by  $x_i = 1$  and then a perspective<sup>2</sup> is applied. However,  $R_i$  may only reach a part of the face. See, for example, Figure 3. In this regard, we would like to make two points:

- It can be tempting to extend  $R_i$  to, say,  $\{x \in [0, 1]^n : x_i \geq x_j \forall j\}$ , and thus take the perspective function on the whole face. However, this may lead to a function that does not overestimate  $f$ . We illustrate this in Figure 5. Thus, it is important to consider the “right” subset of the face to take the perspective function.
- Computing envelopes exclusively over box domains helps make the recursive formula cleaner. Moreover, from Lemma 3, we know that on  $x_i = 1$  the envelope must be equal to  $\text{conc}(f_{-i}, [0, 1]^{n-1})$ . As it turns out, due to the structure we consider here, we have something stronger for our case. In Lemma 8 we show that  $\text{conc}(f_{-i}, [0, 1]^{n-1}) = \text{conc}(f_{-i}, R_i \cap \{x : x_i = 1\})$ . This will be beneficial in our arguments since it will help us establish that we are actually obtaining a concave envelope in each region separately.

---

<sup>2</sup>The perspective of a function  $f : \mathbb{R}^n \rightarrow \mathbb{R}$  is  $\tilde{f} : \mathbb{R}^{n+1} \rightarrow \mathbb{R}$  defined as  $\tilde{f}(x, z) = zf(x/z)$  for  $z > 0$  and  $\tilde{f}(x, 0) = 0$ . One of its key properties is that it preserves the convexity/concavity of  $f$  [73].



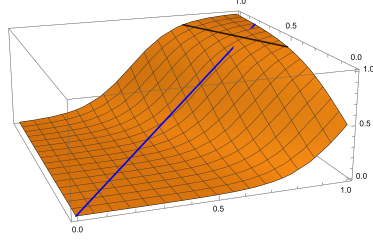


**Fig. 5:** Illustration of why taking the perspective over a complete face of  $\text{conc}(f, [0, 1]^n)$  does not yield a valid overestimator. The function  $f(x)$  of Example 1 is plotted in orange. The black line is  $w^\top x + b = \hat{z}$ . The blue ray represents taking the perspective onto a point that lies on  $R_f$ , which goes “into” the graph of the function  $f(x)$ .

The following lemma will be useful to prove Lemma 8.

**Lemma 7.** *Let  $\hat{z}$  be the tie point of  $\sigma$  in  $[b, w^\top \mathbf{1} + b]$ , and define the region  $R_i$  according to Definition 3. If  $R_i \neq \emptyset$ , then  $e_i \in R_i$ , where  $e_i$  is the  $i$ -th canonical vector. In particular, this implies  $w_i + b < \hat{z}$ .*

*Proof.* Take  $x \in R_i$ . Clearly  $x \neq 0$ . Then we can take  $\tilde{x} = x/\|x\|_\infty$  which satisfies  $w^\top \tilde{x} + b < \hat{z}$ . Additionally,  $\tilde{x}_i = 1$ , thus

$$\hat{z} - b > w^\top \tilde{x} \geq w_i = w^\top e_i$$

This shows the result.  $\square$

**Lemma 8.** *Let  $\hat{z}$  be the tie point of  $\sigma$  in  $[b, w^\top \mathbf{1} + b]$ , and suppose  $R_i \neq \emptyset$ . Then*

$$\text{conc}(f_{-i}, [0, 1]^{n-1}) = \text{conc}(f_{-i}, [0, 1]^{n-1} \cap \{x_{-i} : w_{-i}^\top x_{-i} + w_i + b \leq \hat{z}\})$$

$$\text{on } [0, 1]^{n-1} \cap \{x_{-i} : w_{-i}^\top x_{-i} + w_i + b \leq \hat{z}\}.$$

Before moving to the proof, let us provide some intuition on this lemma. Consider Figure 3(b): what Lemma 8 states is that if we restrict the function until the black point, the envelope we obtain is the same as if we consider the complete interval. This is, essentially, because the tie point that yields the envelope on the slice (red points on Figure 3(b)) is always on the left of the black point. This simple fact is what the proof formalizes.

*Proof.* Note that

$$f_{-i}(x_{-i}) = \sigma(w_{-i}^\top x_{-i} + w_i + b)$$

thus, the domain of  $\sigma$  in this case is  $[w_i + b, w^\top \mathbf{1} + b]$ . Recall that the domain of  $\sigma$  in  $f(x)$  is  $[b, w^\top \mathbf{1} + b]$ . Let  $\hat{z}^{-i}$  be the tie point of  $\sigma$  in  $[w_i + b, w^\top \mathbf{1} + b]$ . Since by Lemma 7 we have  $w_i + b < \hat{z}$ , we can apply Lemma 2 (case 3) to obtain

$$\hat{z} \geq \hat{z}^{-i}.$$

To conclude, we apply Lemma 6 to  $f_{-i}$  to obtain

$$\text{conc}(f_{-i}, [0, 1]^{n-1}) = \text{conc}(f_{-i}, [0, 1]^{n-1} \cap \{x_{-i} : w_{-i}^\top x_{-i} + w_i + b \leq \hat{z}\}).$$

□

## 5 Concave envelope proof

To alleviate notation in the proofs, we will assume in this section  $f(0) = \sigma(b) = 0$ . This can be achieved by defining  $\sigma'(z) = \sigma(z) - \sigma(b)$ ; clearly  $\sigma$  satisfies STFE if and only if  $\sigma'$  does, and computing the envelope of  $\sigma'(w^\top x + b)$  is equivalent to computing the envelope of  $\sigma(w^\top x + b)$  (modulo a translation).

### 5.1 Overestimator definition

We begin by defining the candidate for concave envelope.

**Definition 4.** Consider  $w \in \mathbb{R}_+^n$ ,  $b \in \mathbb{R}$  and let  $f : [0, 1]^n \rightarrow \mathbb{R}$  be a function of the form  $f(x) = \sigma(w^\top x + b)$  where  $\sigma$  satisfies the STFE property and  $\sigma(b) = 0$ . Then, we define

$$g(x) = \begin{cases} f(x) & \text{if } x \in R_f \\ \frac{\sigma(\hat{z})}{\hat{z}-b}(w^\top x) & \text{if } x \in R_l \\ x_i \text{conc}(f_{-i}, [0, 1]^{n-1}) \left( \frac{x_{-i}}{x_i} \right) & \text{if } x \in R_i, i = 1, \dots, n \end{cases}$$

where  $R_f, R_l$  and  $R_i$  are defined using Definition 3 with  $\hat{z}$  as the tie point of  $\sigma$  in  $[b, w^\top \mathbf{1} + b]$ .

We note the following details about  $g$ :

- The function  $g$  is well-defined at 0, since it is covered by one of the first two cases.
- Some of the regions may be empty, which is not an issue. For instance, if  $b \geq \hat{z}$ , then  $g = f$ .
- As mentioned earlier, the third case is nothing but the perspective of  $\text{conc}(f_{-i}, [0, 1]^{n-1})(x_{-i})$ .

We will show the function  $g$  is precisely the concave envelope of  $f$  in  $[0, 1]^n$ . Our strategy will be to use induction on the dimension  $n$ .

### 5.2 General properties of the envelope candidate

**Lemma 9.** Consider  $g$  as in Definition 4. Then,  $g$  is continuous on  $[0, 1]^n$ .

*Proof.* Firstly, the function  $g$  is equal to  $h$  in  $R_f \cup R_l$ , which we know is concave. Thus, it is continuous in  $R_f \cup R_l$ . In each  $R_i$  individually, the function is concave (thus continuous) since it is the perspective of a concave function [73]. In  $x = 0$ , all different pieces evaluate to 0.

If we take  $x \in \text{cl}(R_f) \cap \text{cl}(R_i)$ , with  $x \neq 0$ , we have

$$\hat{z} \geq w^\top \frac{x}{\|x\|_\infty} + b \geq w^\top x + b \geq \hat{z}.$$

Since  $w \in \mathbb{R}_+^n$  and  $x \neq 0$ ,  $w^\top x \neq 0$  and thus  $\|x\|_\infty = 1$ . This implies  $x_i = 1$  and

$$x_i \text{conc}(f_{-i}, [0, 1]^{n-1})(x_{-i}/x_i) = f_{-i}(x_{-i}) = f(x).$$

where the first equality follows from the same argument in the proof of Lemma 8 (i.e., the tie point used in  $f_{-i}$  is smaller than  $\hat{z}$ ). Thus, both definitions in  $R_f$  and  $R_i$  coincide.

If we take  $x \in \text{cl}(R_l) \cap \text{cl}(R_i)$ , with  $x \neq 0$ , we have

$$w^\top \frac{x}{\|x\|_\infty} + b = \hat{z}$$

and  $x/\|x\|_\infty \in \text{cl}(R_l) \cap \text{cl}(R_i)$ . Therefore, the definition on  $R_l$  evaluated on  $x/\|x\|_\infty$  is

$$\frac{\sigma(\hat{z})}{\hat{z} - b}(w^\top x/\|x\|_\infty) = \sigma(\hat{z}),$$

and the definition on  $R_i$  evaluated on  $x/\|x\|_\infty$  is

$$\text{conc}(f_{-i}, [0, 1]^{n-1})(x_{-i}/\|x\|_\infty) = f_{-i}(x_{-i}/\|x\|_\infty) = f(x/\|x\|_\infty),$$

where the first equality follows from the same argument in the proof of Lemma 8. Note that  $f(x/\|x\|_\infty) = \sigma(w^\top x/\|x\|_\infty + b) = \sigma(\hat{z})$  and thus

$$\frac{\sigma(\hat{z})}{\hat{z} - b}(w^\top x/\|x\|_\infty) = \text{conc}(f_{-i}, [0, 1]^{n-1})(x_{-i}/\|x\|_\infty)$$

We conclude this case by noting that both functions definitions on  $R_l$  and  $R_i$  are linear on the rays, and thus the equality holds after rescaling the arguments.

The last case to consider is  $x \in \text{cl}(R_i) \cap \text{cl}(R_j)$  for  $i \neq j$ . In this case, we must have  $x_i = x_j = \|x\|_\infty$ , and

$$\text{Def. on } R_i \longrightarrow x_i \text{conc}(f_{-i}, [0, 1]^{n-1})(x_{-i}/\|x\|_\infty)$$

$$\text{Def. on } R_j \longrightarrow x_j \text{conc}(f_{-j}, [0, 1]^{n-1})(x_{-j}/\|x\|_\infty)$$

Since both the  $i$  and  $j$  component of  $x/\|x\|_\infty$  are 1, we can use Lemma 3 twice to obtain

$$\text{conc}(f_{-i}, [0, 1]^{n-1})(x_{-i}/\|x\|_\infty) = \text{conc}((f_{-i})_{-j}, [0, 1]^{n-2})((x_{-i})_{-j}/\|x\|_\infty)$$

$$\begin{aligned}
&= \text{conc}((f_{-j})_{-i}, [0, 1]^{n-2}) ((x_{-j})_{-i}/\|x\|_\infty) \\
&= \text{conc}(f_{-j}, [0, 1]^{n-1}) (x_{-j}/\|x\|_\infty)
\end{aligned}$$

Since  $x_i = x_j$ , we conclude the result.  $\square$

**Lemma 10.** *Consider  $g$  as in Definition 4. Then,  $g$  is an overestimator of  $f$ .*

*Proof.* In  $R_l \cup R_f$  it follows since here  $g(x) = h(x)$ , which we know is an overestimator.

Let us now consider  $x \in R_i$  fixed and consider  $\lambda \geq 0$ . Since in  $R_i$  the function  $g$  is defined as the perspective of  $\text{conc}(f_{-i}, [0, 1]^{n-1})$ , we have

$$g(\lambda x) = \lambda g(x) \quad \forall \lambda \geq 0$$

Moreover,  $g(0) = 0 = f(0)$  and  $g(x/\|x\|_\infty) = \text{conc}(f_{-i}, [0, 1]^{n-1}) (x_{-i}/\|x\|_\infty) \geq f(x/\|x\|_\infty)$ , therefore,  $\alpha(\lambda) := g(\lambda x/\|x\|_\infty)$  defines an overestimator of the secant  $\beta(\lambda) = \lambda f(x/\|x\|_\infty)$  for  $\lambda \in [0, 1]$ .

We conclude by noting that the one-dimensional function

$$\gamma(\lambda) := f(\lambda x/\|x\|_\infty) = \sigma(\lambda w^\top x/\|x\|_\infty + b)$$

satisfies the STFE property since  $w^\top x/\|x\|_\infty > 0$ . Note that the argument of  $\sigma$  ranges in  $[b, w^\top x/\|x\|_\infty + b]$ , and  $w^\top x/\|x\|_\infty + b < \hat{z}$  since  $x \in R_i$ . Thus, by Lemma 2 (case 2),  $\text{conc}(\gamma, [0, 1])(\lambda) = \lambda\gamma(1)$ . In particular,

$$\underbrace{f(\lambda x/\|x\|_\infty)}_{\gamma(\lambda)} \leq \underbrace{\lambda f(x/\|x\|_\infty)}_{\lambda\gamma(1)=\beta(\lambda)} \leq \underbrace{g(\lambda x/\|x\|_\infty)}_{\alpha(\lambda)}$$

for every  $\lambda \in [0, 1]$ . The results follows since  $\|x\|_\infty \leq 1$ .  $\square$

**Lemma 11.** *The function  $g$  defined as in Definition 4 is concave in each region. Moreover,  $g$  is the concave envelope of each region separately.*

*Proof.* Concavity in each region follows because  $f$  is concave on  $R_f$ ,  $g$  is linear on  $R_l$ , and on each  $R_i$  is the perspective of a concave function.

To show that it is the concave envelope in each region, we argue case by case.

In  $R_f \cup R_l$ ,  $g(x) = h(x)$  where  $h$  is defined in Definition 4 and we know  $h$  is the envelope in these regions (Lemma 5). The fact that it is actually the envelope in  $R_f$  and  $R_l$  separately follows from the same proof as in Lemma 5.

For  $R_i$ , the argument is similar. In this case,

$$\begin{aligned}
g(x) &= x_i \text{conc}(f_{-i}, [0, 1]^{n-1})(x_{-i}/x_i) && \text{(definition of } g) \\
&= x_i \text{conc}(f, [0, 1]^n \cap R_i \cap \{x_i = 1\})(x/x_i) && \text{(Lemma 8)}
\end{aligned}$$

$$\begin{aligned} &\leq x_i \text{conc}(f, R_i)(x/x_i) + (1 - x_i) \text{conc}(f, R_i)(0) \quad (\text{conc}(f, R_i)(0) \geq f(0) = 0) \\ &\leq \text{conc}(f, R_i)(x) \end{aligned}$$

Since  $g$  is also an overestimator and concave in  $R_i$ , we conclude it must be the concave envelope.  $\square$

Finally, we state a lemma whose proof follows directly from the definition of  $g$ .

**Lemma 12.** *For every  $x \in [0, 1]^n$ , either*

1.  $g(x) = f(x)$ , or
2.  $g(x)$  is linear on the segment  $[0, x]$ .

With these results, we are ready to proceed to the main proof: that  $g$  is concave in  $[0, 1]^n$ . Note that this suffices to show that  $g$  is the concave envelope, as we already established that it is the envelope in each region separately. As mentioned earlier, we prove this by induction on the dimension  $n$ .

### 5.3 Global concavity: Base case

This case is simple: for  $n = 1$ , since  $\|x\|_\infty = x$  the regions become

$$\begin{aligned} R_f &:= \{x \in [0, 1] : wx + b \geq \hat{z}\} \\ R_l &:= \{x \in [0, 1] : wx + b < \hat{z}, wx + bx \geq \hat{z}x\} \\ R_1 &:= \{x \in [0, 1] : wx + bx < \hat{z}x\} \end{aligned}$$

By definition,  $\hat{z} \in [b, w + b]$ , and thus  $R_1 = \emptyset$ . Therefore, in this case, we recover the envelope formula given by the STFE property (after the translation and scaling  $wx + b$ ).

### 5.4 Global concavity: Inductive step

Now we assume that for dimensions  $n - 1$  and lower, the concave envelope of a function of the form  $\sigma(w^\top x + b)$  can be expressed using the formula of  $g$  as in Definition 4.

Our strategy to prove the concavity of  $g$  in  $n$  dimensions is as follows. Since we have established continuity of  $g$  on the hypercube (Lemma 9), we can focus on establishing concavity on the interior of the hypercube, and thus we consider  $x \in (0, 1)^n$  arbitrary. We will show that for any  $y$  in a dense subset of the hypercube (to be determined), we have

$$f(x) \leq g(y) + \nabla g(y)(x - y). \quad (3)$$

Why this suffices? If  $y$  is fixed, and we let  $x$  vary within an arbitrary region (not necessarily the same as  $y$ ), then the right-hand side of (3) defines a linear overestimator of  $f$  on the region of  $x$ ; however,  $g$  is the envelope on any region separately (Lemma 11), and thus we would get  $g(x) \leq g(y) + \nabla g(y)(x - y)$  for  $x, y$  in a dense subset of the hypercube. Using the continuity of  $g$  in the hypercube and concavity in each region, we can conclude.

To prove (3), we begin by reducing the cases we have to analyze. If  $x, y$  are in the same region, the result clearly follows by concavity in each region (Lemma 11). If  $y \in R_l \cup R_f$ , since in these regions  $g(y) = h(y)$ , and we know  $h$  is a global concave overestimator of  $f$  (Lemma 4), we have

$$f(x) \leq h(y) + \nabla h(y)(x - y) = g(y) + \nabla g(y)(x - y)$$

for any  $x \in [0, 1]^n$ . Therefore, we reduce to consider the case of  $y \in R_i$  for some  $R_i$ : moreover, we can consider  $y \in \text{int}(R_i)$  by density.

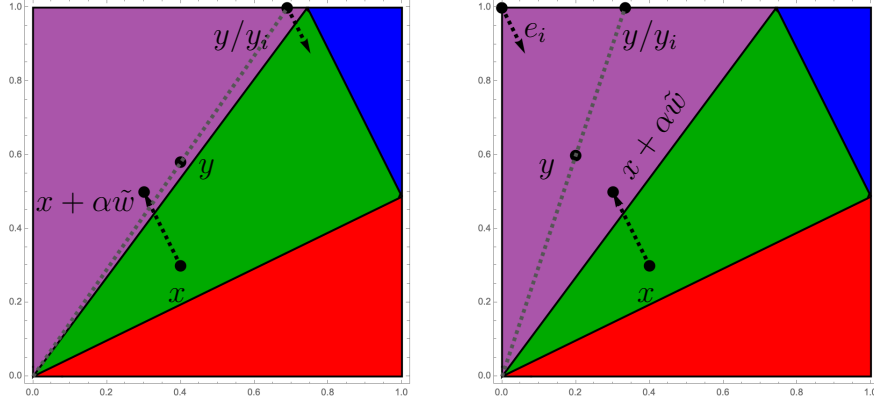
The last case we can discard is when  $x \in R_f$ : by the proof of Lemma 9, we see that the intersection of  $\text{cl}(R_i) \cap \text{cl}(R_f)$  is on the boundary of the hypercube. From this, we see that it suffices to show (3) holds for  $y$  in a dense subset of  $\text{int}(R_i)$  and  $x \notin (R_i \cup R_f)$ .

Before showing the proof, let us describe the high-level strategy of it. Consider Figure 6, where  $R_i$  is the purple region; here, we display two possible “locations” for  $y$  within  $R_i$ , which will become clearer next. We note that these figures follow the same parameters as in Example 1, and thus the reader can use previous figures for a more detailed analysis.

The strategy we follow is to first find a direction  $\tilde{w}$  that is orthogonal to  $w$ , and that can move  $x$  into  $R_i$ . The advantage of this orthogonality is that the function  $f$  stays constant. Then, since  $x + \alpha\tilde{w} \in R_i$ , we can use the concavity of  $g$  over  $R_i$  to overestimate  $g(x + \alpha\tilde{w})$  with a gradient on  $y$ . This gradient-based overestimation could potentially not overestimate the function in  $x$ , so the next step is to prove that it indeed works. To do so, we analyze  $\nabla g(y)$ : this gradient is almost completely determined by  $\nabla(\text{conc}(f_{-i}, [0, 1]^{n-1}))(y/y_i)$ , thus, we will separate the two cases described Lemma 12 depending on  $y/y_i$ . We will provide further details on this case distinction in the proof.

As a last comment on the high-level strategy, the two-dimensional picture may suggest that one could always consider  $x \in R_l$ . However, this is not the case in general: in higher dimensions, non-trivial intersections of regions  $R_i$  and  $R_j$  for  $i \neq j$  could appear. Moreover, in the convex case in two dimensions,  $R_l$  is empty, and the  $R_1$  and  $R_2$  regions do intersect in the interior of the box.

We begin by showing that such a  $\tilde{w}$  always exists. While in two dimensions, it is fairly simple to see this, in higher dimensions, one needs to be more careful.



(a) Illustration in the case  $y/y_i$  is such that  $g(y/y_i) = f(y/y_i)$ . (b) Illustration in the case  $y/y_i$  is such that  $g(y/y_i) \neq f(y/y_i)$ .

**Fig. 6:** Illustration of proof strategy for inductive step in concavity of  $g$ . Here,  $R_i$  is the purple region. In both cases, the dashed arrows are pointing in opposite directions and are orthogonal to  $w$ .

**Lemma 13.** Let  $\tilde{y} \in R_i$  for some  $i$  such that  $\tilde{y}_i = 1$  and  $\tilde{y}_j < 1$  for  $j \neq i$ , and  $x \in (0, 1)^n \setminus (R_f \cup R_i)$ . There exists  $\tilde{w} \in \mathbb{R}^n$  such that

1.  $\tilde{w}^\top w = 0$
2.  $x + \alpha \tilde{w} \in R_i$  for some  $\alpha \geq 0$
3.  $\tilde{y} - \varepsilon \tilde{w} \in R_i$  for some  $\varepsilon > 0$

*Proof.* We first note that if there exists such  $\tilde{y}$ , then  $e_i \in R_i$  by Lemma 7. The proof follows using a case distinction.

**Case 1.**

If  $w^\top e_i \geq w^\top x$ , then we consider  $\lambda \leq 1$  such that  $w^\top(\lambda e_i) = w^\top x$  and define

$$\tilde{w} = \lambda e_i - x$$

and  $\alpha = 1$ . Then,  $\tilde{w}^\top w = 0$  by construction and since  $w^\top x + b < \hat{z}$  we have that  $x + \tilde{w} = \lambda e_i \in R_i$ .

To show  $\tilde{y} - \varepsilon \tilde{w} \in R_i$  we proceed as follows. Note that

$$w_i x_i < w^\top x = \lambda w_i \Rightarrow x_i < \lambda$$

The  $i$ -th component of  $\tilde{y} - \varepsilon \tilde{w}$  is

$$1 - \varepsilon(\lambda - x_i)$$

and the rest is

$$\tilde{y}_j + \varepsilon x_j$$

Since  $\lambda > x_i$  and  $\tilde{y}_j < 1$  for  $j \neq i$ , we can ensure that for  $\varepsilon$  small  $\tilde{y} - \varepsilon \tilde{w} \in [0, 1]^n$ , and that the  $i$ -th component is strictly larger than the rest. Finally,

$$w^\top \frac{(\tilde{y} - \varepsilon \tilde{w})}{1 - \varepsilon(\lambda - x_i)} - (\hat{z} - b) \xrightarrow{\varepsilon \rightarrow 0} w^\top \tilde{y} - (\hat{z} - b) < 0$$

Thus, for  $\varepsilon$  small enough,

$$w^\top \frac{(\tilde{y} - \varepsilon \tilde{w})}{\|\tilde{y} - \varepsilon \tilde{w}\|_\infty} < \hat{z} - b.$$

We conclude  $\tilde{y} - \varepsilon \tilde{w} \in R_i$ .

**Case 2.**

If  $w^\top e_i < w^\top x$ , then we consider  $\lambda > 1$  such that  $w^\top(\lambda e_i) = w^\top x$  and, as before, define

$$\tilde{w} = \lambda e_i - x.$$

We will now need to make use of  $\alpha \neq 1$ : take

$$\alpha = \frac{1 - x_i}{\lambda - x_i}$$

Note that  $\alpha \in (0, 1)$  since  $x_i < 1 < \lambda$ .

In this case,  $\tilde{w}^\top w = 0$  again follows by construction. To show that  $x + \alpha \tilde{w} \in R_i$ , note that

$$\begin{aligned} (x + \alpha \tilde{w})_i &= 1 \\ (x + \alpha \tilde{w})_j &= (1 - \alpha)x_j \end{aligned}$$

therefore  $x + \alpha \tilde{w} \in [0, 1]^n$ ,  $\|x + \alpha \tilde{w}\|_\infty = 1$ , and additionally

$$w^\top(x + \alpha \tilde{w}) = w^\top x < \hat{z} - b$$

thus  $x + \alpha \tilde{w} \in R_i$ .

Finally, and similarly to the previous case, the  $i$ -th component of  $\tilde{y} - \varepsilon \tilde{w}$  is

$$1 - \varepsilon(\lambda - x_i)$$

and the rest is

$$\tilde{y}_j + \varepsilon x_j$$



In this case, we also have  $\lambda > x_i$ , and since  $\tilde{y}_j < 1$  for  $j \neq i$ , we can ensure that for  $\varepsilon$  small, the  $i$ -th component of  $\tilde{y} - \varepsilon\tilde{w}$  is the largest. Finally,

$$w^\top \frac{(\tilde{y} - \varepsilon\tilde{w})}{1 - \varepsilon(\lambda - x_i)} - (\hat{z} - b) \xrightarrow{\varepsilon \rightarrow 0} w^\top \tilde{y} - (\hat{z} - b) < 0$$

Thus, for  $\varepsilon$  small enough,

$$w^\top \frac{(\tilde{y} - \varepsilon\tilde{w})}{\|\tilde{y} - \varepsilon\tilde{w}\|_\infty} < \hat{z} - b$$

We conclude  $\tilde{y} - \varepsilon\tilde{w} \in R_i$ .  $\square$

The last piece of information we need for the final proof is the gradient of  $g$  on the interior of a region  $R_i$ . Let us define

$$g_{ave,-i} = \text{conc}(f_{-i}, [0, 1]^{n-1})$$

Then,

$$\begin{aligned} \frac{\partial}{\partial x_j} g(x) &= \frac{\partial}{\partial x_j} (x_i g_{ave,-i}(x_{-i}/x_i)) = \frac{\partial}{\partial x_j} g_{ave,-i}(x_{-i}/x_i) & j \neq i \\ \frac{\partial}{\partial x_i} g(x) &= \frac{\partial}{\partial x_i} (x_i g_{ave,-i}(x_{-i}/x_i)) \\ &= g_{ave,-i}(x_{-i}/x_i) - \nabla g_{ave,-i}(x_{-i}/x_i)^\top \begin{pmatrix} x_{-i} \\ x_i \end{pmatrix} \end{aligned}$$

We proceed to the main part of the global concavity proof.

**Lemma 14.** *Inequality (3) holds for every  $y$  in a dense subset of  $R_i$  and every  $x \in (0, 1)^n \setminus (R_i \cup R_f)$ .*

*Proof.* We consider  $y \in \text{int}(R_i)$  such that  $g_{ave,-i}$  is differentiable in  $y_{-i}/y_i$ . This induces a dense subset of  $\text{int}(R_i)$  since  $g_{ave,-i}$  is differentiable almost everywhere. Moreover,  $g$  is differentiable in  $y$ . Note that in this case,  $1 > y_i > y_j > 0$  for every  $j \neq i$ . We take  $\tilde{w}$  as in Lemma 13 (we leave which  $\tilde{y}$  we use ambiguous for now since it depends on a case distinction below). Then

$$\begin{aligned} f(x) &= f(x + \alpha\tilde{w}) & (w^\top \tilde{w} = 0) \\ &\leq g(x + \alpha\tilde{w}) & (g \text{ overest. in } R_i) \\ &\leq g(y) + \nabla g(y)^\top (x + \alpha\tilde{w} - y) & (g \text{ concave in } R_i \text{ and diff. at } y) \\ &= g(y) + \nabla g(y)^\top (x - y) + \alpha \nabla g(y)^\top \tilde{w} \end{aligned}$$

Therefore, it suffices to show  $\nabla g(y)^\top \tilde{w} \leq 0$ . We refer the reader to Figure 6 for a picture reference of these steps.

By induction,  $\text{conc}(f_{-i} - f_{-i}(0), [0, 1]^{n-1})$  can be described using a function of the form of  $g$ . Following the notation preceding this lemma, we have

$$\text{conc}(f_{-i} - f_{-i}(0), [0, 1]^{n-1}) = g_{ave,-i} - f_{-i}(0).$$

We can apply Lemma 12 to  $g_{ave,-i} - f_{-i}(0)$  and note that  $y_{-i}/y_i$  must be in one of two cases.

**Case 1 in Lemma 12.**

In this case the envelope is tight at  $y_{-i}/y_i$ , i.e.,  $g_{ave,-i}(y_{-i}/y_i) - f_{-i}(0) = f_{-i}(y_{-i}/y_i) - f_{-i}(0)$ . Recall that

$$f_{-i}(y_{-i}/y_i) - f_{-i}(0) = f(y/y_i) - f(e_i)$$

For this case, we choose  $\tilde{w}$  for  $\tilde{y} := y/y_i$  in Lemma 13. With this, we move in  $-\tilde{w}$  from  $y/y_i$ : this corresponds to the case of Figure 6(a). This yields,

$$\begin{aligned} f(y/y_i) &= f(y/y_i - \varepsilon\tilde{w}) && (w^\top \tilde{w} = 0) \\ &\leq g(y/y_i - \varepsilon\tilde{w}) && (g \text{ overest. in } R_i) \\ &\leq g(y) + \nabla g(y)^\top (y/y_i - \varepsilon\tilde{w} - y) && (g \text{ concave in } R_i \text{ and diff. in } y) \\ &= g(y) + \nabla g(y)^\top (y/y_i - y) - \varepsilon \nabla g(y)^\top \tilde{w} \\ &= g(y/y_i) - \varepsilon \nabla g(y)^\top \tilde{w} && (g \text{ linear on the rays in } R_i) \\ &= \text{conc}(f_{-i}, [0, 1]^{n-1})(y_{-i}/y_i) - \varepsilon \nabla g(y)^\top \tilde{w} && (\text{definition of } g) \\ &= g_{ave,-i}(y_{-i}/y_i) - \varepsilon \nabla g(y)^\top \tilde{w} \\ &= f_{-i}(y_{-i}/y_i) - \varepsilon \nabla g(y)^\top \tilde{w} && (\text{case definition}) \\ &= f(y/y_i) - \varepsilon \nabla g(y)^\top \tilde{w} \end{aligned}$$

This proves  $\nabla g(y)^\top \tilde{w} \leq 0$ .

**Case 2 in Lemma 12.**

Since we are assuming  $g_{ave,-i}$  is differentiable in  $y_{-i}/y_i$ , this case can be stated as

$$g_{ave,-i}(y_{-i}/y_i) - f_{-i}(0) = \nabla g_{ave,-i}(y_{-i}/y_i)^\top y_{-i}/y_i$$

Note that in the previous case, we heavily relied on the envelope being tight for  $y/y_i$ , which may not be the case here. However, since  $g_{ave,-i}$  is linear in a ray, we can move linearly to a point that is always tight:  $e_i$ . Therefore, for this case, we choose  $\tilde{w}$  for  $\tilde{y} := e_i$  in Lemma 13 and move in  $-\tilde{w}$ : this corresponds to the case of Figure 6(b). This yields,

$$f(e_i) = f(e_i - \varepsilon\tilde{w}) \quad (w^\top \tilde{w} = 0)$$

$$\begin{aligned}
&\leq g(e_i - \varepsilon \tilde{w}) && (g \text{ overest. in } R_i) \\
&\leq g(y) + \nabla g(y)^\top (e_i - \varepsilon \tilde{w} - y) && (g \text{ concave in } R_i \text{ and diff. in } y) \\
&= g(y) + \nabla g(y)^\top (e_i - y) - \varepsilon \nabla g(y)^\top \tilde{w}
\end{aligned}$$

Let us analyze the product  $\nabla g(y)^\top (e_i - y)$ . Recall that

$$\begin{aligned}
\frac{\partial}{\partial x_j} g(x) &= \frac{\partial}{\partial x_j} g_{ave,-i}(x_{-i}/x_i) && j \neq i \\
\frac{\partial}{\partial x_i} g(x) &= g_{ave,-i}(x_{-i}/x_i) - \nabla g_{ave,-i}(x_{-i}/x_i)^\top \begin{pmatrix} x_{-i} \\ x_i \end{pmatrix}
\end{aligned}$$

Thus,

$$\begin{aligned}
\nabla g(y)^\top (e_i - y) &= -\nabla g_{ave,-i}(y_{-i}/y_i)^\top y_{-i} \\
&\quad + (1 - y_i) \left( g_{ave,-i}(y_{-i}/y_i) - \nabla g_{ave,-i}(y_{-i}/y_i)^\top \begin{pmatrix} y_{-i} \\ y_i \end{pmatrix} \right) \\
&= (1 - y_i) g_{ave,-i}(y_{-i}/y_i) - \nabla g_{ave,-i}(y_{-i}/y_i)^\top \begin{pmatrix} y_{-i} \\ y_i \end{pmatrix}
\end{aligned}$$

Also recall that  $g(y) = y_i g_{ave,-i}(y_{-i}/y_i)$ , thus

$$\begin{aligned}
f(e_i) &\leq g_{ave,-i}(y_{-i}/y_i) - \nabla g_{ave,-i}(y_{-i}/y_i)^\top \begin{pmatrix} y_{-i} \\ y_i \end{pmatrix} - \varepsilon \nabla g(y)^\top \tilde{w} \\
&= f_{-i}(0) - \varepsilon \nabla g(y)^\top \tilde{w} && (\text{case definition}) \\
&= f(e_i) - \varepsilon \nabla g(y)^\top \tilde{w}
\end{aligned}$$

This implies  $\nabla g(y)^\top \tilde{w} \leq 0$ . □

## 6 Computational experiments

### 6.1 Envelope comparison in simple examples

To provide a first evaluation of the concave envelope, we implemented a Python routine to evaluate the formula given in Theorem 1 for the sigmoid function  $\sigma(x) = 1/(1+e^{-x})$ , and compare it against the baseline overestimator given by  $h$  in Lemma 4.

To quantify the improvement of  $\text{conc}(f, [0, 1]^n)$  with respect to  $h$ , we use the *total gap* (see [74]) between  $h$  and  $f$  defined as

$$\delta^h := \int_{[0,1]^n} (h(x) - f(x)) dx$$

Similarly, we define  $\delta^{\text{conc}(f,[0,1]^n)}$ , and with this we define the gap improvement as

$$\text{Gap Improvement} = \frac{\delta^h - \delta^{\text{conc}(f,[0,1]^n)}}{\delta^h}.$$

We estimate the integrals using Monte Carlo integration.

For the parameters defined in Example 1, we obtain

$$\int_{[0,1]^2} f(x)dx \approx 0.2811, \quad \int_{[0,1]^2} h(x)dx \approx 0.5616, \quad \int_{[0,1]^2} \text{conc}(f, [0, 1]^n)(x)dx \approx 0.5218.$$

which yields a gap improvement of 14.18%.

We also considered a 3-dimensional example, defined by parameters  $b = -8$  and  $w = [5, 8, 7]$ . In this case, we obtain

$$\int_{[0,1]^3} f(x)dx \approx 0.5226, \quad \int_{[0,1]^3} h(x)dx \approx 0.8216, \quad \int_{[0,1]^3} \text{conc}(f, [0, 1]^n)(x)dx \approx 0.7323.$$

which yields a gap improvement of 29.86%.

While these are only two simple examples, they illustrate that the global improvements given by the envelopes can be considerable with respect to the  $h$  overestimator.

## 6.2 Envelopes in computations of activation bounds

In this section, we evaluate the use of the envelopes in the computation of *activation bounds*, defined as follows. For a given neuron  $v$  and a network input  $x \in \mathcal{X}$ , let  $\text{NN}_v(x)$  be the value of the input to  $v$  when propagating  $x$ . This corresponds to the value of one of the  $a$  variables in (1). We say  $\ell_v$  is an activation lower bound if

$$\min_{x \in \mathcal{X}} \text{NN}_v(x) \geq \ell_v \tag{4}$$

We similarly define an activation upper bound  $u_v$ . Computing strong activation bounds is crucial when approximating the behavior of a neural network, as they can help to tighten the convex approximations of it. Computing the tightest bounds, however, can be computationally intractable. For more background on activations bounds and their importance, we refer the reader to [6, 7, 15, 75].

Note that using a convex relaxation of  $\text{NN}_v(x)$  in (4), as described in this article, yields valid activation bounds. In these experiments, we compare two relaxation techniques: one given by the  $h$  overestimator, as defined in Lemma 4, and the concave envelope of Theorem 1. These define concave overestimators of  $\sigma(w^\top x + b)$ , but one can also use these strategies for convex underestimators as discussed in Section 3.3.

### ***Cutting plane algorithm***

To evaluate the effect of the envelopes described in this paper, we follow a cutting plane approach to approximate on-the-fly the convex hulls of the sets  $\{(x, y) \in D \times \mathbb{R} : y = \sigma(w^\top x + b)\}$  for each neuron. Fix a neuron  $v$  in layer  $i$ , and suppose we have computed activation bounds  $\ell, u$  up to layer  $i - 1$ . The cutting plane algorithm to compute an activation *lower* bound for  $v$  proceeds as follows.

1. We start with a base linear relaxation of the system (1) (described below) up to neuron  $v$ . We minimize  $a_v^i$  over this relaxation to obtain an initial activation bound  $\ell_v$ .
2. For a given solution  $(\bar{a}, \bar{h})$ , we check if there exists a neuron  $\eta$  in a layer  $j < i$  such that

$$(\bar{h}_\eta^j, \bar{h}^{(j-1)}) \notin \text{conv} \left( \left\{ (z, y) \in \mathbb{R} \times D_{j-1} : z = \sigma \left( W_\eta^{(j-1)\top} y + b_\eta^{(j-1)} \right) \right\} \right), \quad (5)$$

where  $W_\eta^{(j-1)}$  is the vector of weights going into  $\eta$ , and  $D_{j-1}$  are valid bounds for the  $h^{(j-1)}$  variables. When the activation functions are non-decreasing, we can take

$$D_{j-1} = [\sigma(\ell^{j-1}), \sigma(u^{j-1})]$$

where  $\ell^{j-1}$  and  $u^{j-1}$  is the vector of all activations bounds of layer  $j - 1$ , and  $\sigma$  is applied component-wise.

We check (5) using our recursive formula for the envelopes and, if possible, we compute a cutting plane on variables  $(h_\eta^j, h^{(j-1)})$ . We repeat the procedure for every neuron of the previous layers.

3. We add all cutting planes and solve the new relaxation.
4. We go back to step 2 until a stopping criterion is met and output a valid bound for  $a_v^i$ .

The algorithm for computing activation upper bounds works analogously.

Note that this algorithm describes the use of the concave/convex envelopes, but we can also use the—potentially looser but simpler—overestimator  $h$ . This defines two settings: ENV when we use the  $n$ -dimensional envelopes and H-EST when we use the  $h$  estimator. We remind the reader that the  $h$  estimator is based on the one-dimensional envelope of the activation function, as done in [20].

### ***Implementation and Hardware***

We implemented the cutting plane algorithm in Python, using SCIP [76] through the PySCIPOpt [77] interface, with SoPlex 6.0.3 as the LP solver. All experiments were run single-threaded on a Windows machine with a Ryzen 5 5600X 3.7 GHz CPU and 16 GB RAM.

### ***Stopping Criteria***

We limit the rounds of cutting planes to 20 per bound computation. This means that when we visit a node  $v$  in layer  $i$  to compute activation bounds, we run at most 20

cut rounds for the minimization of  $a_v^i$ , and 20 cut rounds for the maximization. For a fixed  $v$ , each round of cuts may add one cut per neuron of the previous layers.

Our second stopping criterion is related to stalling. If the value of  $a_v^i$  does not change more than  $10^{-5}$ , we stop the cut generation.

### *Instances*

We tested the cutting plane algorithm in 6 fully connected neural networks, trained on the MNIST dataset [78] using PyTorch [79]. These networks have: an input layer, 5 or 6 hidden layers, and an output layer. All hidden layers have 5 neurons, except for the last one which has 10 neurons. Between the last hidden layer and the output, a softmax function is applied.

In terms of the activations, we considered three types. Firstly, two S-shaped activations: the sigmoid activation  $\sigma(x) = 1/(1 + e^{-x})$  and the SELU activation

$$\sigma(x) = \lambda \begin{cases} x, & x > 0 \\ \alpha(\exp(x) - 1), & x \leq 0 \end{cases}$$

with  $\lambda$  and  $\alpha$  defined in Table 2. We also considered a convex activation function: the ELU, which is defined using the same formula as the SELU, but with  $\lambda = 1$  and  $\alpha \leq 1$ . In our case, we used  $\alpha = 1$ . We chose these activations to obtain a variety of cases: one bounded S-shaped, one unbounded S-shaped, and one convex. All networks were trained using an  $\ell_2$  regularization with parameter 0.005.

We name these networks as ACT\_X\_Y, where ACT indicates the activation, X the number of hidden layers, and Y the number of nodes in each hidden layer. For example, Sigmoid\_6\_5.

Since the first hidden layer does not have an activation function on the previous layer, the differences in the bound computations produced by different convexifications can only be seen from hidden layer 2 onwards. This means that the cutting plane algorithm is executed 50 or 60 times (one per bound per neuron in layers 2–6), where each run consists of at most 20 rounds of cuts.

### *Initial Relaxation*

In our setting,  $\mathcal{X} = [0, 1]^{784}$ , since the input is given by a vector of pixel intensities of a  $28 \times 28$  grayscale image. From this, we can propagate initial activation bounds using interval arithmetic (see, e.g., [75]).

Removing the equalities of the form  $y = \sigma(z)$  in (1) provides a rough initial linear relaxation, but we can refine it slightly using the following simple estimators of  $y = \sigma(z)$ . If the activation bounds of a neuron are  $[\ell, u]$ , and  $\sigma$  is convex on a sub-interval of  $[\ell, u]$ , we overestimate  $\sigma$  using the inequality given by the secant of the STFE property. If  $\sigma$  is concave in  $[\ell, u]$ , we impose  $y \leq \max_{z \in [\ell, u]} \sigma(z)$ , which can be efficiently computed. The initial underestimators are defined analogously.

### *Evaluation Metric*

Our main evaluation metric is the improvement over the initial activation bounds. For a neuron  $v$  in layer  $i$ , if the initial lower bound is  $\ell_v$ , and after running a cutting plane

algorithm (either ENV or H-EST) we obtain  $\tilde{\ell}_v$ , the improvement is

$$\frac{\tilde{\ell}_v - \ell_v}{|\ell_v|}.$$

We define the improvement for the upper bounds similarly.

### **Results**

In Table 3, we present a summary of our results. For all instances, and for hidden layers 2, 5, and 6, we show the average improvement of ENV or H-EST with respect to the initial relaxation of the activation lower and upper bounds.

The results of Table 3 show that in every instance, and every layer, ENV is at least as good as H-EST: while this was expected and seems trivial, cutting planes can behave unpredictably when there is a limited budget. How better ENV performed heavily depends on the activation.

In the sigmoid instances, the improvements of ENV over H-EST, if any, are very minor. The largest improvement was roughly 2.8%, which is not computationally significant. We believe that this is due to the boundedness of the sigmoid function. In our experiments, the main benefit of a refined convexification is to propagate better activations bounds that can further refine deeper convexifications and, thus, better activation bounds in deeper layers. When we propagate previous activation bounds, the activation function plays a significant role in which domains are used to convexify (see  $D_{j-1}$  in (5)). In the presence of a function like the sigmoid activation, an improvement on an activation bound would be dampened by the application of the activation.

In the SELU instances, the story changes dramatically. In layers 5 and 6, we see that ENV is 13%-23% better than H-EST in most cases, which is significant. In layer 2, the improvements are smaller: most are close to 5%, which reinforces our previous claim that envelope convexification can be more beneficial in deeper layers. As opposed to the sigmoid, the SELU function does not diminish the potential improvements made on the activation bounds. It is slightly surprising, in a good way, that already on layer 2, the improvements of ENV over H-EST are better in the SELU than in the sigmoid.

In the ELU instances, the results are comparable to those of the SELU, although in layer 6 the improvements are more modest. In layer 6, ENV is 5%-6% better than H-EST, while in layer in 5 the improvements of ENV over H-EST are between 10%-24%. In layer 2, the improvements of ENV are between 5%-9%, which is better than in the SELU case.

Overall, we observe that significant improvements can be obtained using the envelopes we developed here, in comparison to simply using the one-dimensional envelope of the activation.

**Table 3:** Comparison of H-EST and ENV in the computation of activation bounds for layers 2, 5, and 6 of our instances. Starting from column 2, all entries are the average improvements of H-EST and ENV with respect to the base relaxation on the activation lower or upper bound for a given layer.

Instance	Layer 2 - H-EST		Layer 2 - ENV		Layer 5 - H-EST		Layer 5 - ENV		Layer 6 - H-EST		Layer 6 - ENV	
	lb imp.	ub imp.	lb imp.	ub imp.	lb imp.	ub imp.	lb imp.	ub imp.	lb imp.	ub imp.	lb imp.	ub imp.
Sigmoid_5.5	57.8%	52.5%	57.8%	52.5%	46.3%	71.0%	47.1%	72.4%	-	-	-	-
Sigmoid_6.5	41.9%	69.1%	41.9%	69.1%	57.9%	59.9%	59.0%	62.7%	47.5%	71.9%	48.3%	73.0%
SELU_5.5	49.5%	33.6%	54.3%	40.8%	69.0%	87.4%	84.8%	93.7%	-	-	-	-
SELU_6.5	54.8%	19.9%	59.6%	33.3%	75.2%	46.7%	89.4%	69.2%	53.8%	78.1%	73.9%	91.4%
ELU_5.5	35.4%	17.9%	40.7%	26.6%	34.4%	56.5%	58.7%	75.4%	-	-	-	-
ELU_6.5	43.7%	49.5%	50.9%	54.0%	77.1%	76.6%	88.2%	87.2%	81.4%	86.5%	86.5%	93.2%



## 7 Conclusions

In this paper, we have derived a formula for the concave envelope of  $\sigma(w^\top x + b)$  over a box domain, where  $\sigma$  satisfies the STFE property. This includes convex, concave, and S-shaped functions. The envelope is described using a recursive formula that requires at most  $n$  one-dimensional envelope computations in order to (i) evaluate the  $n$ -dimensional envelope and (ii) construct a supergradient of it. This envelope formula can be used in the convexification of trained neural networks by providing a way of checking

$$(\hat{x}, \hat{y}) \in \text{conv}(\{(x, y) \in D \times \mathbb{R} : y = \sigma(w^\top x + b)\}),$$

and constructing a separating hyperplane if one exists. This effectively convexifies an activation together with the affine function that precedes it. Our framework is flexible enough to be easily applied in neural networks with many different types of activation functions.

Our computational results indicate that there can be significant gains in using the  $n$ -dimensional envelope instead of using a one-dimensional envelope (i.e., using the  $h$  overestimator). In particular, in the deeper layers of networks with SELU and ELU activations, we observed that the  $n$ -dimensional envelopes were considerably better than the one-dimensional envelopes.

In the sigmoid activation, however, no significant differences were observed between ENV and H-EST. We believe the main reason is the boundedness of the sigmoid function; however, we do not know if this is the only reason.

Overall, we believe our envelope computation can be of great help in the incorporation of trained neural networks in optimization routines. Future steps include using these envelopes in other optimization problems, computational improvements, and including more activation functions of the same layer. In particular, we believe that our formula can be combined with the existing approaches that convexify groups of neurons simultaneously, in order to further strengthen their multi-neuron constraints.

## Acknowledgements

We would like to thank Felipe Serrano for his helpful feedback on an early version of this article. We would also like to thank Joey Huchette, Mohit Tawarmalani, and Calvin Tsay for their valuable comments.

## References

- [1] Cheng, C.-H., Nührenberg, G., Ruess, H.: Maximum resilience of artificial neural networks. In: International Symposium on Automated Technology for Verification and Analysis, pp. 251–268 (2017). Springer
- [2] Fischetti, M., Jo, J.: Deep neural networks and mixed integer linear optimization. *Constraints* **23**(3), 296–309 (2018) <https://doi.org/10.1007/s10601-018-9285-6>

- [3] Khalil, E.B., Gupta, A., Dilkina, B.: Combinatorial attacks on binarized neural networks. In: International Conference on Learning Representations (ICLR) (2019)
- [4] Tjeng, V., Xiao, K., Tedrake, R.: Evaluating Robustness of Neural Networks with Mixed Integer Programming. arXiv (2017) <https://doi.org/10.48550/arXiv.1711.07356>
- [5] Li, L., Xie, T., Li, B.: Sok: Certified robustness for deep neural networks. In: 2023 IEEE Symposium on Security and Privacy (SP), pp. 94–115 (2022). IEEE Computer Society
- [6] Liu, C., Arnon, T., Lazarus, C., Strong, C., Barrett, C., Kochenderfer, M.J., *et al.*: Algorithms for verifying deep neural networks. *Foundations and Trends® in Optimization* **4**(3-4), 244–404 (2021)
- [7] Zhao, H., Hijazi, H., Jones, H., Moore, J., Tanneau, M., Van Hentenryck, P.: Bound tightening using rolling-horizon decomposition for neural network verification. In: International Conference on the Integration of Constraint Programming, Artificial Intelligence, and Operations Research, pp. 289–303 (2024). Springer
- [8] Serra, T., Tjandraatmadja, C., Ramalingam, S.: Bounding and counting linear regions of deep neural networks. In: International Conference on Machine Learning (ICML), pp. 4558–4566 (2018). PMLR
- [9] Serra, T., Ramalingam, S.: Empirical bounds on linear regions of deep rectifier networks. In: AAAI Conference on Artificial Intelligence (AAAI) (2020)
- [10] Cai, J., Nguyen, K.-N., Shrestha, N., Good, A., Tu, R., Yu, X., Zhe, S., Serra, T.: Getting away with more network pruning: From sparsity to geometry and linear regions. In: International Conference on the Integration of Constraint Programming, Artificial Intelligence, and Operations Research (CPAIOR) (2023)
- [11] Serra, T., Kumar, A., Ramalingam, S.: Lossless compression of deep neural networks. In: 17th International Conference on Integration of Constraint Programming, Artificial Intelligence, and Operations Research (CPAIOR), pp. 417–430 (2020). Springer
- [12] Serra, T., Yu, X., Kumar, A., Ramalingam, S.: Scaling up exact neural network compression by ReLU stability. *Advances in neural information processing systems* **34**, 27081–27093 (2021)
- [13] ElAraby, M., Wolf, G., Carvalho, M.: OAMIP: Optimizing ANN architectures using mixed-integer programming. In: International Conference on the Integration of Constraint Programming, Artificial Intelligence, and Operations Research (CPAIOR) (2023)

- [14] Perakis, G., Tsiourvas, A.: Optimizing objective functions from trained relu neural networks via sampling. arXiv:2205.14189 (2022)
- [15] Tong, J., Cai, J., Serra, T.: Optimization over trained neural networks: Taking a relaxing walk (2023)
- [16] Gurobi Optimization, LLC: Gurobi Machine Learning (2024). <https://www.gurobi.com/features/gurobi-machine-learning/>
- [17] Turner, M., Chmiela, A., Koch, T., Winkler, M.: Pyscipopt-ml: Embedding trained machine learning models into mixed-integer programs. arXiv preprint arXiv:2312.08074 (2023)
- [18] Huchette, J., Muñoz, G., Serra, T., Tsay, C.: When deep learning meets polyhedral theory: A survey. arXiv preprint arXiv:2305.00241 (2023)
- [19] Schweidtmann, A.M., Mitsos, A.: Deterministic global optimization with artificial neural networks embedded. *Journal of Optimization Theory and Applications* **180**(3), 925–948 (2019)
- [20] Wilhelm, M.E., Wang, C., Stuber, M.D.: Convex and concave envelopes of artificial neural network activation functions for deterministic global optimization. *Journal of Global Optimization* **85**(3), 569–594 (2023)
- [21] Salman, H., Yang, G., Zhang, H., Hsieh, C.-J., Zhang, P.: A convex relaxation barrier to tight robustness verification of neural networks. *Advances in Neural Information Processing Systems* **32** (2019)
- [22] Singh, G., Ganvir, R., Püschel, M., Vechev, M.: Beyond the single neuron convex barrier for neural network certification. *Advances in Neural Information Processing Systems* **32** (2019)
- [23] Müller, M.N., Makarchuk, G., Singh, G., Püschel, M., Vechev, M.: Prima: general and precise neural network certification via scalable convex hull approximations. *Proceedings of the ACM on Programming Languages* **6**(POPL), 1–33 (2022)
- [24] Ferrari, C., Mueller, M.N., Jovanović, N., Vechev, M.: Complete verification via multi-neuron relaxation guided branch-and-bound. In: *International Conference on Learning Representations* (2022). <https://openreview.net/forum?id=LamHf1oaK>
- [25] Zhang, H., Wang, S., Xu, K., Li, L., Li, B., Jana, S., Hsieh, C.-J., Kolter, J.Z.: General cutting planes for bound-propagation-based neural network verification. *Advances in Neural Information Processing Systems* (2022)
- [26] Tang, X., Zheng, Y., Liu, J.: Boosting multi-neuron convex relaxation for neural network verification. In: *International Static Analysis Symposium*, pp. 540–563

(2023). Springer

- [27] Ma, Z., Li, J., Bai, G.: Relu hull approximation. *Proceedings of the ACM on Programming Languages* **8**(POPL), 2260–2287 (2024)
- [28] Roth, K.: A primer on multi-neuron relaxation-based adversarial robustness certification. In: *ICML 2021 Workshop on Adversarial Machine Learning*
- [29] Anderson, R., Huchette, J., Ma, W., Tjandraatmadja, C., Vielma, J.P.: Strong mixed-integer programming formulations for trained neural networks. *Mathematical Programming* **183**(1), 3–39 (2020)
- [30] Ehlers, R.: Formal verification of piece-wise linear feed-forward neural networks. In: *Automated Technology for Verification and Analysis: 15th International Symposium, ATVA 2017, Pune, India, October 3–6, 2017, Proceedings 15*, pp. 269–286 (2017). Springer
- [31] Kronqvist, J., Misener, R., Tsay, C.: Between steps: Intermediate relaxations between big-M and convex hull formulations. In: *International Conference on the Integration of Constraint Programming, Artificial Intelligence, and Operations Research (CPAIOR)* (2021)
- [32] Tsay, C., Kronqvist, J., Thebelt, A., Misener, R.: Partition-based formulations for mixed-integer optimization of trained ReLU neural networks. In: *Neural Information Processing Systems (NeurIPS)*, vol. 34 (2021)
- [33] Kronqvist, J., Misener, R., , Tsay, C.: P-split formulations: A class of intermediate formulations between big-M and convex hull for disjunctive constraints. *arXiv:2202.05198* (2022)
- [34] Bastani, O., Ioannou, Y., Lampropoulos, L., Vytiniotis, D., Nori, A., Criminisi, A.: Measuring neural net robustness with constraints. *Advances in neural information processing systems* **29** (2016)
- [35] Sildir, H., Aydin, E.: A mixed-integer linear programming based training and feature selection method for artificial neural networks using piece-wise linear approximations. *Chemical Engineering Science* **249**, 117273 (2022)
- [36] Benussi, E., Patane, A., Wicker, M., Laurenti, L., Kwiatkowska, M.: Individual fairness guarantees for neural networks. *arXiv preprint arXiv:2205.05763* (2022)
- [37] Dvijotham, K., Stanforth, R., Goyal, S., Mann, T.A., Kohli, P.: A dual approach to scalable verification of deep networks. In: *UAI*, vol. 1, p. 3 (2018)
- [38] Raghunathan, A., Steinhardt, J., Liang, P.S.: Semidefinite relaxations for certifying robustness to adversarial examples. *Advances in neural information processing systems* **31** (2018)

- [39] Wei, D., Wu, H., Wu, M., Chen, P.-Y., Barrett, C., Farchi, E.: Convex bounds on the softmax function with applications to robustness verification. In: International Conference on Artificial Intelligence and Statistics, pp. 6853–6878 (2023). PMLR
- [40] McCormick, G.P.: Computability of global solutions to factorable nonconvex programs: Part i—convex underestimating problems. *Mathematical programming* **10**(1), 147–175 (1976)
- [41] Al-Khayyal, F.A., Falk, J.E.: Jointly constrained biconvex programming. *Mathematics of Operations Research* **8**(2), 273–286 (1983) <https://doi.org/10.1287/moor.8.2.273>
- [42] Tardella, F.: On the existence of polyhedral convex envelopes. *Frontiers in Global Optimization*, 563–573 (2004) [https://doi.org/10.1007/978-1-4613-0251-3\\_30](https://doi.org/10.1007/978-1-4613-0251-3_30)
- [43] Tardella, F.: Existence and sum decomposition of vertex polyhedral convex envelopes. *Optimization Letters* **2**(3), 363–375 (2008) <https://doi.org/10.1007/s11590-007-0065-2>
- [44] Meyer, C.A., Floudas, C.A.: Convex envelopes for edge-concave functions. *Mathematical Programming* **103**(2), 207–224 (2005) <https://doi.org/10.1007/s10107-005-0580-9>
- [45] Rikun, A.D.: A convex envelope formula for multilinear functions. *Journal of Global Optimization* **10**(4), 425–437 (1997) <https://doi.org/10.1023/A:1008217604285>
- [46] Sherali, H.D.: Convex envelopes of multilinear functions over a unit hypercube and over special discrete sets. *Acta Mathematica Vietnamica* **22**(1), 245–270 (1997)
- [47] Ryoo, H.S., Sahinidis, N.V.: Analysis of bounds for multilinear functions. *Journal of Global Optimization* **19**(4), 403–424 (2001) <https://doi.org/10.1023/A:1011295715398>
- [48] Meyer, C.A., Floudas, C.A.: Trilinear monomials with mixed sign domains: Facets of the convex and concave envelopes. *Journal of Global Optimization* **29**(2), 125–155 (2004) <https://doi.org/10.1023/B:JOGO.0000042112.72379.e6>
- [49] Bao, X., Sahinidis, N.V., Tawarmalani, M.: Multiterm polyhedral relaxations for nonconvex, quadratically constrained quadratic programs. *Optimization Methods & Software* **24**(4-5), 485–504 (2009) <https://doi.org/10.1080/10556780902883184>
- [50] Luedtke, J., Namazifar, M., Linderoth, J.: Some results on the strength of relaxations of multilinear functions. *Mathematical Programming* **136**(2), 325–351 (2012) <https://doi.org/10.1007/s10107-012-0606-z>

- [51] Tawarmalani, M., Richard, J.-P.P., Xiong, C.: Explicit convex and concave envelopes through polyhedral subdivisions. *Mathematical Programming* **138**(1), 531–577 (2013) <https://doi.org/10.1007/s10107-012-0581-4>
- [52] Sherali, H.D., Alameddine, A.: An explicit characterization of the convex envelope of a bivariate bilinear function over special polytopes. *Annals of Operations Research* **25**(1), 197–209 (1990) <https://doi.org/10.1007/BF02283695>
- [53] Zamora, J.M., Grossmann, I.E.: A branch and contract algorithm for problems with concave univariate, bilinear and linear fractional terms. *Journal of Global Optimization* **14**(3), 217–249 (1999) <https://doi.org/10.1023/A:1008312714792>
- [54] Tawarmalani, M., Sahinidis, N.V.: Semidefinite relaxations of fractional programs via novel convexification techniques. *Journal of Global Optimization* **20**(2), 133–154 (2001) <https://doi.org/10.1023/A:1011233805045>
- [55] Kuno, T.: A branch-and-bound algorithm for maximizing the sum of several linear ratios. *Journal of Global Optimization* **22**(1), 155–174 (2002) <https://doi.org/10.1023/A:1013807129844>
- [56] Benson, H.P.: On the construction of convex and concave envelope formulas for bilinear and fractional functions on quadrilaterals. *Computational Optimization and Applications* **27**(1), 5–22 (2004) <https://doi.org/10.1023/B:COAP.0000004976.52180.7f>
- [57] Linderoth, J.: A simplicial branch-and-bound algorithm for solving quadratically constrained quadratic programs. *Mathematical Programming* **103**(2), 251–282 (2005) <https://doi.org/10.1007/s10107-005-0582-7>
- [58] Anstreicher, K.M., Burer, S.: Computable representations for convex hulls of low-dimensional quadratic forms. *Mathematical Programming* **124**(1), 33–43 (2010) <https://doi.org/10.1007/s10107-010-0355-9>
- [59] Hijazi, H.: Perspective envelopes for bilinear functions. In: *AIP Conference Proceedings*, vol. 2070, p. 020017 (2019). AIP Publishing LLC
- [60] Locatelli, M., Schoen, F.: On convex envelopes for bivariate functions over polytopes. *Mathematical Programming* **144**(1), 65–91 (2014) <https://doi.org/10.1007/s10107-012-0616-x>
- [61] Locatelli, M.: Polyhedral subdivisions and functional forms for the convex envelopes of bilinear, fractional and other bivariate functions over general polytopes. *Journal of Global Optimization* **66**(4), 629–668 (2016) <https://doi.org/10.1007/s10898-016-0418-4>
- [62] Locatelli, M.: Convex envelopes of bivariate functions through the solution of KKT systems. *Journal of Global Optimization* **72**(2), 277–303 (2018) <https://doi.org/10.1007/s10898-018-0000-0>

[doi.org/10.1007/s10898-018-0626-1](https://doi.org/10.1007/s10898-018-0626-1)

- [63] Muller, B., Serrano, F., Gleixner, A.: Using two-dimensional projections for stronger separation and propagation of bilinear terms. *SIAM Journal on Optimization* **30**(2), 1339–1365 (2020) <https://doi.org/10.1137/19M1249825>
- [64] Locatelli, M.: Convex envelope of bivariate cubic functions over rectangular regions. *Journal of Global Optimization* **76**(1), 1–24 (2020) <https://doi.org/10.1007/s10898-019-00846-2>
- [65] Liberti, L., Pantelides, C.C.: Convex envelopes of monomials of odd degree. *Journal of Global Optimization* **25**(2), 157–168 (2003) <https://doi.org/10.1023/A:1021924706467>
- [66] Maranas, C.D., Floudas, C.A.: Finding all solutions of nonlinearly constrained systems of equations. *Journal of Global Optimization* **7**, 143–182 (1995)
- [67] Tawarmalani, M., Sahinidis, N.V.: Convex extensions and envelopes of lower semi-continuous functions. *Mathematical Programming* **93**(2), 247–263 (2002)
- [68] Jach, M., Michaels, D., Weismantel, R.: The convex envelope of  $(n-1)$ -convex functions. *SIAM Journal on Optimization* **19**(3), 1451–1466 (2008) <https://doi.org/10.1137/07069359X>
- [69] Khajavirad, A., Sahinidis, N.V.: Convex envelopes of products of convex and component-wise concave functions. *Journal of Global Optimization* **52**(3), 391–409 (2012) <https://doi.org/10.1007/s10898-011-9747-5>
- [70] Khajavirad, A., Sahinidis, N.V.: Convex envelopes generated from finitely many compact convex sets. *Mathematical Programming* **137**(1), 371–408 (2013) <https://doi.org/10.1007/s10107-011-0496-5>
- [71] Barrera, J., Moreno, E., Muñoz, G.: Convex envelopes for ray-concave functions. *Optimization Letters* **16**(8), 2221–2240 (2022)
- [72] Sahlodin, A.M.: Global optimization of dynamic process systems using complete search methods. PhD thesis (2013)
- [73] Günlük, O., Linderoth, J.: Perspective reformulation and applications. In: Lee, J., Leyffer, S. (eds.) *Mixed Integer Nonlinear Programming*, pp. 61–89. Springer, New York, NY (2012)
- [74] Khajavirad, A., Michalek, J.J., Sahinidis, N.V.: Relaxations of factorable functions with convex-transformable intermediates. *Mathematical Programming* **144**(1), 107–140 (2014)
- [75] Badilla, F., Goycoolea, M., Muñoz, G., Serra, T.: Computational trade-offs of optimization-based bound tightening in relu networks. arXiv preprint

arXiv:2312.16699 (2023)

- [76] Bolusani, S., Besançon, M., Bestuzheva, K., Chmiela, A., Dionísio, J., Donkiewicz, T., Doornmalen, J., Eifler, L., Ghannam, M., Gleixner, A., Graczyk, C., Halbig, K., Hedtke, I., Hoen, A., Hojny, C., Hulst, R., Kamp, D., Koch, T., Kofler, K., Lentz, J., Manns, J., Mexi, G., Mühmer, E., Pfetsch, M.E., Schlösser, F., Serrano, F., Shinano, Y., Turner, M., Vigerske, S., Weninger, D., Xu, L.: The SCIP Optimization Suite 9.0. Technical report, Optimization Online (February 2024). <https://optimization-online.org/2024/02/the-scip-optimization-suite-9-0/>
- [77] Maher, S., Miltenberger, M., Pedroso, J.P., Rehfeldt, D., Schwarz, R., Serrano, F.: PySCIPOpt: Mathematical programming in python with the SCIP optimization suite. *Mathematical Software – ICMS 2016*, 301–307 (2016) [https://doi.org/10.1007/978-3-319-42432-3\\_37](https://doi.org/10.1007/978-3-319-42432-3_37)
- [78] Deng, L.: The mnist database of handwritten digit images for machine learning research. *IEEE Signal Processing Magazine* **29**(6), 141–142 (2012)
- [79] Paszke, A., Gross, S., Massa, F., Lerer, A., Bradbury, J., Chanan, G., Killeen, T., Lin, Z., Gimelshein, N., Antiga, L., et al.: Pytorch: An imperative style, high-performance deep learning library. *Advances in neural information processing systems* **32** (2019)
- [80] Rockafellar, R.T.: *Convex Analysis*. Princeton Mathematical Series. Princeton University Press, Princeton, N. J. (1970)



## A Functions that satisfy STFE

**Lemma 15.** *If a function  $\sigma$  is either convex, concave, or S-shaped, then it satisfies the STFE property.*

*Proof.* The concave and convex cases are direct. Let us consider  $\sigma$  S-shaped and  $[\ell, u] \subseteq \mathbb{R}$  arbitrary. If  $[\ell, u]$  is contained in either the convex or concave regions of  $\sigma$ , we are done. Thus we assume  $\sigma$  is convex in  $[\ell, \tilde{z}]$  and concave in  $[\tilde{z}, u]$  for some  $\tilde{z} \in (\ell, u)$ .

Firstly, note that there must be  $\hat{z} \geq \tilde{z}$  such that  $\text{conc}(\sigma, [\ell, u])$  is affine on  $[\ell, \hat{z}]$ . Moreover,

$$\text{conc}(\sigma, [\ell, u])(\ell) = \sigma(\ell), \quad \text{conc}(\sigma, [\ell, u])(\hat{z}) = \sigma(\hat{z}).$$

See e.g. [67]. If  $\hat{z} = u$ , we are done. Otherwise,  $\hat{z} \in (\ell, u)$ , and in this case the directional derivatives of  $\text{conc}(\sigma, [\ell, u])$  at  $\hat{z}$  are well-defined. We can thus use [67, Theorem 4] to show that there exists a supergradient  $\xi$  such that

$$\sigma(x) \leq \sigma(\hat{z}) + \xi(x - \hat{z})$$

for all  $x \in [\ell, u]$ . Since  $\sigma$  is concave in  $[\tilde{z}, u]$ , we can take supergradients in any point  $z \in [\hat{z}, u]$ ; these will have non-increasing slope (see [80, Theorem 24.1]) and thus they define a valid overestimator of  $\sigma$  on the whole interval  $[\ell, u]$ . Thus,

$$\text{conc}(\sigma, [\ell, u])(x) = \sigma(x) \quad \forall x \in [\hat{z}, u].$$

□

## B Proof of Lemma 2

### *Decreasing upper bound, case 1.*

This result follows directly since  $\text{conc}(\sigma, [L, U])$  defines a concave overestimator in  $[L, \tilde{U}]$ , which is linear in  $[L, \hat{z}]$ , equal to  $\sigma$  in  $\{L, \hat{z}\}$ , and also equal to  $\sigma$  for  $z \geq \hat{z}$ . The fact that  $\hat{z}$  is the tie point for  $[L, \tilde{U}]$  follows by definition.

### *Increasing lower bound*

We note that  $\text{conc}(\sigma, [L, U])$  defines a valid overestimator of  $\sigma$  over  $[\tilde{L}, U]$  which is equal to  $\sigma$  in  $[\hat{z}, U]$ . Therefore,  $\text{conc}(\sigma, [\tilde{L}, U])$  must be equal to  $\sigma$  in  $[\hat{z}, U]$  as well. This directly implies that the tie point over  $[\tilde{L}, U]$  must be less or equal than  $\hat{z}$ .

### *Decreasing upper bound, case 2.*

In this case we are considering  $\tilde{U} \in [L, \hat{z}]$ . We assume  $L < \hat{z}$ ; otherwise, the result is trivial.

Let  $\tilde{z}$  be the tie point in  $[L, \tilde{U}]$ . If  $\tilde{z} = \tilde{U}$ , we are done, thus we assume  $\tilde{z} < \tilde{U}$ , which implies  $\sigma$  is concave in  $[\tilde{z}, \tilde{U}]$  and the latter has nonempty interior.

Let  $[m, M] \supseteq [\tilde{z}, \tilde{U}]$  be a maximal interval where  $\sigma$  is concave. We claim that  $M \leq \hat{z}$ . Otherwise,  $\sigma$  is concave on  $[\tilde{z}, \hat{z} + \varepsilon]$  for some  $\varepsilon > 0$  and we get that

$$\begin{cases} \text{conc}(\sigma, [L, \tilde{U}])(z) & \text{if } z \in [L, \tilde{z}) \\ \sigma(z) & \text{if } z \in [\tilde{z}, U] \end{cases}$$

is a valid concave overestimator of  $\sigma$  on  $[L, U]$ , which would imply the tie point in  $[L, U]$  is less or equal than  $\tilde{z} < \hat{z}$ . Moreover, this implies  $\sigma$  is not concave in  $[M - \delta, M + \varepsilon]$  for any  $\delta, \varepsilon > 0$ . Additionally, this implies that the tie point in  $[L, M]$  must be  $\tilde{z}$ .

By definition of  $M$  and the STFE property,  $\text{conc}(\sigma, [m, M + \varepsilon])$  is an affine function in  $[m, M]$  (there could potentially be a tie point in  $[M, M + \varepsilon]$  since the function could have a concave portion in this interval): this affine function is tight at  $m$  and at a point in  $[M, M + \varepsilon]$ . Taking  $\varepsilon \rightarrow 0$ , we obtain an affine function overestimating  $\sigma$  in  $[m, M]$  which is tight at the endpoints. Since  $\sigma$  is concave in this interval, we conclude that  $\sigma$  must be *affine* in  $[m, M]$ . Let  $\Lambda(z)$  be this affine function, and note that it must define an overestimator of  $\sigma$  on  $[L, M]$ , since we know that the tie point of  $\sigma$  in  $[L, M]$  is  $\tilde{z} \in [m, M)$ .

If  $m \leq L$  we are done, so we assume  $m > L$ . Note that in this case, it must hold that  $\tilde{z} = m$ . Moreover, there must exist  $\tilde{L} \in (L, m)$  such that

$$\sigma(\tilde{L}) < \Lambda(\tilde{L}).$$

By the ‘‘Increasing lower bound’’ property, the tie point in  $[\tilde{L}, M]$  is  $m$ ; it cannot be strictly smaller since  $\sigma$  is not concave on  $[m - \delta, M]$ . This shows that  $\text{conc}(\sigma, [\tilde{L}, M])$  cannot be an affine function: if it were, it would have to be  $\Lambda$  as  $[m, M]$  has nonempty interior, but we know  $\Lambda$  is not tight at  $\tilde{L}$  and the envelopes are always tight on the endpoints.

To conclude, we consider  $[\tilde{L}, M + \varepsilon]$ . By the same arguments as above,  $\text{conc}(\sigma, [\tilde{L}, M + \varepsilon])$  must be an affine function in  $[\tilde{L}, M]$  which is tight in  $\tilde{L}$  and in some point in  $[M, M + \varepsilon]$ . Letting  $\varepsilon \rightarrow 0$ , we obtain an affine overestimator of  $\sigma$  on  $[\tilde{L}, M]$  which is tight at the endpoints. This is a contradiction.